AD-A149 313 AVERAGING EFFECTS IN MODELS OF THREE-DIMENSIONAL TWO-PHASE FLOWS(U) ARMY BALLISTIC RESEARCH LAB ABERDEEN PROVING GROUND MD A K CELMINS OCT 84 BRL-TR-2598 1/1

UNCLASSIFIED SBI-AD-F300 500 F/G 19/4 NL

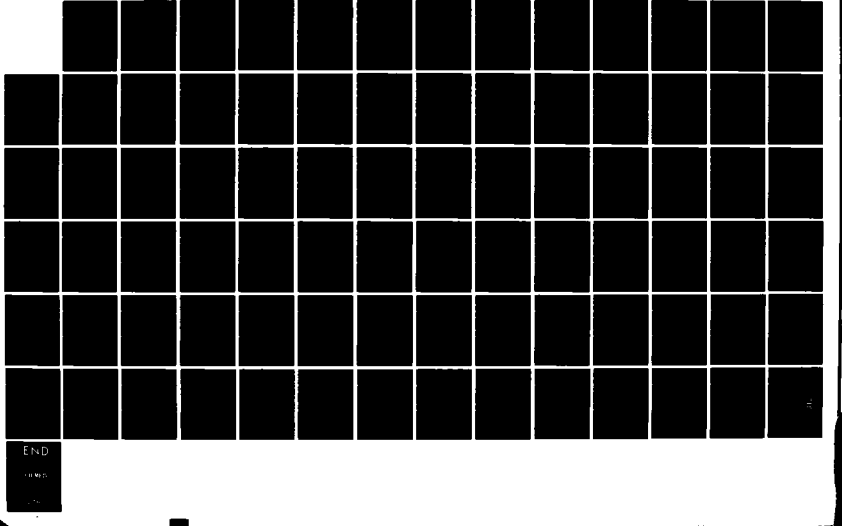

END

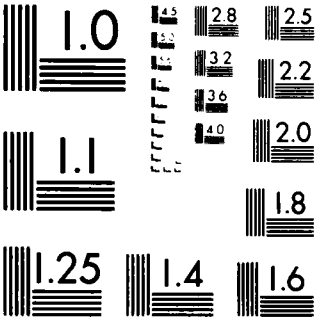

12

AD

BRL

TECHNICAL REPORT BRL-TR-2598

AVERAGING EFFECTS IN MODELS OF THREE-DIMENSIONAL TWO-PHASE FLOWS

Aivars K.R. Celmins

October 1984

US ARMY BALLISTIC RESEARCH LABORATORY
ABERDEEN PROVING GROUND, MARYLAND

Destroy this report when it is no longer needed.
Do not return it to the originator.

Additional copies of this report may be obtained from the National Technical Information Service, U. S. Department of Commerce, Springfield, Virginia 22161.

The findings in this report are not to be construed as an official Department of the Army position, unless so designated by other authorized documents.

The use of trade names or manufacturers' names in this report does not constitute indorsement of any commercial product.

UNCLASSIFIED

SECURITY CLASSIFICATION OF THIS PAGE *(When Data Entered)*

REPORT DOCUMENTATION PAGE		READ INSTRUCTIONS BEFORE COMPLETING FORM
1. REPORT NUMBER Technical Report BRL-TR-2598	2. GOVT ACCESSION NO. AD-A149313	3. RECIPIENT'S CATALOG NUMBER
4. TITLE *(and Subtitle)* Averaging Effects in Models of Three-Dimensional Two-Phase Flows		5. TYPE OF REPORT & PERIOD COVERED 6. PERFORMING ORG. REPORT NUMBER
7. AUTHOR(s) Aivars K. R. Celmins		8. CONTRACT OR GRANT NUMBER(s)
9. PERFORMING ORGANIZATION NAME AND ADDRESS US Army Ballistic Research Laboratory ATTN: AMXBR-IBD Aberdeen Proving Ground, Maryland 21005-5066		10. PROGRAM ELEMENT, PROJECT, TASK AREA & WORK UNIT NUMBERS
11. CONTROLLING OFFICE NAME AND ADDRESS US Army Ballistic Research Laboratory ATTN: AMXBR-OD-ST Aberdeen Proving Ground, Maryland 21005-5066		12. REPORT DATE October 1984 13. NUMBER OF PAGES 82
14. MONITORING AGENCY NAME & ADDRESS*(if different from Controlling Office)*		15. SECURITY CLASS. *(of this report)* UNCLASSIFIED 15a. DECLASSIFICATION/DOWNGRADING SCHEDULE

16. DISTRIBUTION STATEMENT *(of this Report)*

Approved for public release; distribution is unlimited.

17. DISTRIBUTION STATEMENT *(of the abstract entered in Block 20, if different from Report)*

18. SUPPLEMENTARY NOTES

19. KEY WORDS *(Continue on reverse side if necessary and identify by block number)*

Volume Average Interior Ballistics Calculations Lattice Arrangements
Gas-Particle Mixture Undulations of Flow-Undulations Mean Particle Distance
Two-Phase Flow Particle Induced Undulations Neighbor Distance
Gas Volume Fraction Bounds of Undulations Smoothing by Averaging
Particle Aggregate Boundary

20. ABSTRACT *(Continue on reverse side if necessary and identify by block number)*

In order to avoid the treatment of individual particle motion in two-phase flow description, one can use volume averaged descriptors. However, if the averaging volume is too small then individual particles can cause large undulations of the averages. In this report the amplitude of such undulations is estimated by a bound. It is shown that in general, one must average over 30-150 particles in order to obtain reasonably smooth averages. A consequence for interior ballistics calculations is that volume averages

DD FORM 1 JAN 73 1473 EDITION OF 1 NOV 65 IS OBSOLETE

UNCLASSIFIED

SECURITY CLASSIFICATION OF THIS PAGE *(When Data Entered)*

20. ABSTRACT (Continued)

may be used to model the core flow but in general they cannot be used to resolve radial structures in two phases. Also presented are examples of the representation of a gas-particle aggregate boundary in terms of the gas volume fraction, and an approximate expression is derived for the transition curve.

TABLE OF CONTENTS

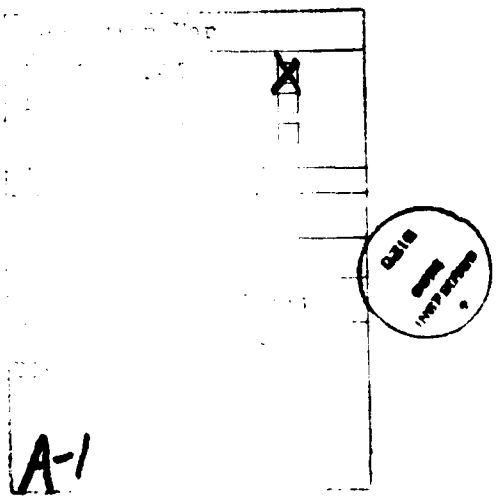

LIST OF FIGURES

LIST OF FIGURES (Continued)

Figures — Page

1. INTRODUCTION

A common method for the derivation of a manageable flow description and of governing equations for flows of gas-particle mixtures is the averaging of local flow properties over a volume.* The averaging produces from the heterogeneous local flow properties smooth flow parameter functions which provide representative descriptions of average properties of the particle aggregate and of the gas between particles. The smoothing is most effective if the averaging volume is so large that the contributions of single particles to the average is negligible. Therefore, it is reasonable to choose a large averaging volume. On the other hand, any volume averaging smoothes, reduces and distorts flow structures particularly those which have an extension smaller than the averaging volume. Hence, in order not to lose flow structures of interest one should choose a small averaging volume. In order to make, under these conditions, a rational choice of the size of the averaging volume one needs a quantitation of the smoothing effect of volume averaging.

In this report a quantitation of the smoothing effect is obtained from an investigation how undulations of the gas volume fraction function α depends on the size and distribution of particles and on the size of the averaging volume. Other flow parameters can be shown to have undulations that are proportional to the undulations of α. The result of the investigation is an estimate of bounds for the undulations of α in terms of the averaging parameters. Using this estimate one can choose a tolerance level for the undulations and obtain a corresponding minimum size of the averaging volume. Flow structures with extensions smaller than the chosen averaging volume are distorted and reduced by the averaging, that is, they are not correctly represented by the average functions.

We illustrate the smoothing of flow structures by considering a plane boundary of a region with uniform particle distribution. In concept, such a boundary is a narrow transition zone between the regions with $\alpha = 1$ (gas only) and $\alpha = \bar{\alpha}$ (the average gas volume fraction in the mixture region). The α obtained by volume averaging has instead a relatively wide transition zone which is spread out over a diameter length of the averaging volume. The width of the transition zone cannot be reduced arbitrarily without penalty, that is, without increasing undulations of the average flow parameters. Hence one has to choose between a smooth representation of the average flow field and an accurate representation of the boundary of the region. The estimated bounds of the undulations can help one to make the choice rationally.

---

*Celmins, Aivars K.R. and Schmitt, James A., *Three-dimensional modeling of gas-combusting solid two-phase flows*, Proceedings of the Third Multi-phase Flow and Heat Transfer Symposium-Workshop, pp. 681-698, Ed., T.N. Veziroglu, 18-20 Apr 1983, Miami Beach, FL.

In Section 2 we present the principal results of the investigation: a quantitative estimate of bounds for particle induced undulations of average flow parameters. Particulars about the derivation of the estimate are given in Section 3. Section 4 provides numerical examples of the representation of a particle aggregate boundary in terms of α. The transition profile can be computed by an approximate formula which is also given in Section 4. All calculations are for a spherical averaging volume and spherical particles arranged in regular three-dimensional lattices. However, by considering different types of lattices we have obtained results that are representative for all regular particle arrangements. Also, the restriction to spherical particles is of little consequence if the particles are small compared to the averaging volume. Section 5 contains a discussion of the results.

2. PRINCIPAL RESULTS

In Section 3 we consider the gas volume fraction α within an averaging sphere with the radius R, and investigate undulations of α due to the location of the sphere. Let the particles be arranged in a regular three-dimensional array, let the particle radius be s, and let $\bar{\alpha}$ be the limit of the gas volume fraction as the averaging sphere becomes infinite. We define a mean distance L_m between the particle centers by

$$L_m = 2s(1 - \bar{\alpha})^{-1/3} \quad . \tag{2.1}$$

A motivation for this definition is given in Appendix B, where it is also shown that L_m is 10-24% larger than the smallest distance between particle centers. If the averaging sphere is finite, then one obtains instead of $\bar{\alpha}$ a value of the gas volume fraction that depends on the position of the sphere. Let $\Delta\bar{\alpha}$ be the difference between an actual value of α and the limit value $\bar{\alpha}$:

$$\Delta\bar{\alpha} = \alpha - \bar{\alpha} \quad . \tag{2.2}$$

$\Delta\bar{\alpha}$ generally depends on the position of the sphere as well as on $\bar{\alpha}$ and L_m/R. In Section 3 we show that its magnitude is bounded by

$$|\Delta\bar{\alpha}| < 0.5\ (1 - \bar{\alpha})\ \bar{\alpha}^2\ (L_m/R)^2 \tag{2.3}$$

independently of the position of the averaging sphere. Eq. (2.3) is based on sample calculations with different lattices for $1 \leq R/L_m \leq 4$ and $0.5 \leq \bar{\alpha} \leq 0.9$. Because the formula also produces the correct limit $\Delta\bar{\alpha} = 0$ for $\bar{\alpha} = 1$, it can be used as an estimate for all $\bar{\alpha} > 0.5$. Extrapolation to

smaller values ($\bar{\alpha} < 0.5$) should be done with reservations, and the same applies to extrapolations to $R/L_m > 4$. The domain $R/L_m < 1$ is of little practical interest because there the undulations are too large.

Eq. (2.3) is graphically displayed in Figure 1 as a relation between a maximum tolerance $|\Delta\bar{\alpha}|_{tol}$ and the corresponding R/L_m which guarantees that the undulations are less than the tolerance. The three curves are shown for $\bar{\alpha} = 0.5$, 0.67 and 0.9, respectively. The value $\bar{\alpha} = 0.67$ is according to Eq. (2.3) the worst case, that is, in this case one needs the largest R/L_m in order to suppress the undulations. The solid lines indicate the domain for which the formula (2.5) was developed and tested by sample calculations. Extrapolations are indicated by dashed lines. Using Figure 1 one obtains, for instance, that the undulations $|\Delta\bar{\alpha}|$ are smaller than 0.01 for $R/L_m > 2.0$ in case $\bar{\alpha} = 0.9$, and for $R/L_m > 2.5$ in case $\bar{\alpha} = 0.5$.

The relation (2.3) also can be expressed in terms of the number N of particles in the averaging volume. To arrive at such an expression we use the approximation

$$N = (2R/L_m)^3 \tag{2.4}$$

(see Eq. (3.5)). Substituting this approximation into Eq. (2.3) one obtains

$$|\Delta\bar{\alpha}| < 2.0\ (1 - \bar{\alpha})\ \bar{\alpha}^2 N^{-2/3} \quad . \tag{2.5}$$

For spherical averaging volumes Eqs. (2.3) and (2.5) are equivalent. However, because the latter also can be used for non-spherical averaging volumes, we shall restrict further discussions to Eq. (2.5). Let $|\Delta\bar{\alpha}|_{tol}$ be a tolerance for the undulations. Then one can reformulate Eq. (2.5) as the following condition for N

$$N > [2\ (1 - \bar{\alpha}\ )]^{3/2}\ \bar{\alpha}^3\ |\Delta\bar{\alpha}|_{tol}^{-3/2} \quad . \tag{2.6}$$

If N satisfies Eq. (2.6) then $|\Delta\bar{\alpha}| < |\Delta\bar{\alpha}|_{tol}$.

If $\bar{\alpha}$ is close to one, then it is reasonable to replace the fixed tolerance by a tolerance level that is a fraction of $1 - \bar{\alpha}$, for instance, by the condition

$$|\Delta\bar{\alpha}| < k\ (1 - \bar{\alpha}) \tag{2.7}$$

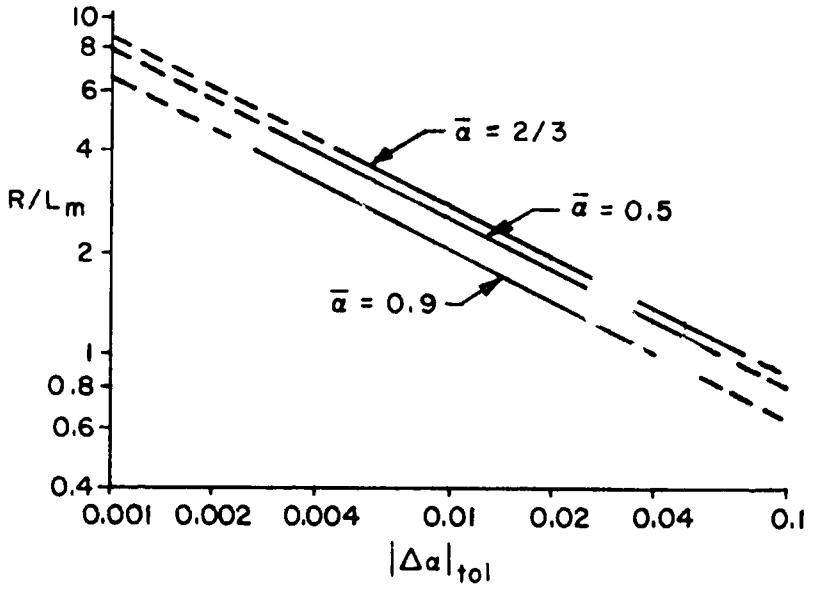

Figure 1. Averaging Sphere Radius for Given Tolerance $|\Delta\bar{\alpha}|_{tol}$

with a proper $k < 1$. The corresponding condition on N is

$$N > (2/k)^{3/2}\, \bar{\alpha}^{3} \quad . \tag{2.8}$$

One may combine both conditions on N by requiring that N should be larger than the maximum of the expressions (2.6) and (2.8). Figure 2 shows the result for $k = 0.2$ and various values of $\bar{\alpha}$. According to that figure, one needs 32-150 particles in order to keep the undulations below the tolerance levels $|\Delta\bar{\alpha}|_{tol} = 0.01$ and $k = 0.2$ within the range $0.7 < \bar{\alpha} < 1.0$. On the other hand, if one is content with the tolerance level $|\Delta\bar{\alpha}|_{tol} = 0.03$ and $k = 0.2$, then 32 particles suffice to represent reasonable average properties.

One can obtain more convenient and less sharp formulas than Eqs. (2.6) and (2.8) by choosing the worst case conditions, namely, $\bar{\alpha} = 2/3$ for Eq. (2.6) and $\bar{\alpha} = 1.0$ for Eq. (2.8). Then the combined condition on N is

$$N > \max\left[\left(\frac{2}{3}\right)^{9/2} |\Delta\bar{\alpha}|_{tol}^{-3/2},\ (2/k)^{3/2}\right] \quad . \tag{2.9}$$

The first argument on the right hand side of Eq. (2.9) corresponds to the rightmost curve in Figure 2. The undulations of averages of other flow parameters, such as gas density, are closely related to the undulations of α. We investigate this relation in Appendix E and show by examples that the amplitude $\Delta\phi$ of particle induced undulations of an average gas property ϕ is proportional to $\Delta\alpha$. If the average has a gradient and changes by $\delta\phi$ along a distance equal to the diameter of the averaging sphere, then

$$|\Delta\phi| \approx |\delta\phi|\,|\Delta\alpha|/(3\alpha) \quad . \tag{2.10}$$

If $\delta\phi = 0$, but there are local particle induced inhomogeneities, then the undulations again are proportional to $\Delta\alpha$ and to the amplitude of the local inhomogeneities. In summary, undulations of α usually induce proportional undulations of other flow parameter averages.

Some consequences of these findings for interior ballistics computations are discussed in Appendix B, where it is shown that the mean distance L_m between particle centers typically is as large as three initial propellant particle diameters. According to Figure 1, the corresponding radius R of the averaging sphere should be larger than six to eight particle diameters (assuming $|\Delta\alpha|_{tol} = 0.01$). This means that a two-phase theory which is based on averaging may not provide correct information about radial flow structures in interior ballistics because the minimum diameter of the averaging sphere is approximately equal to the diameter of the barrel. Such

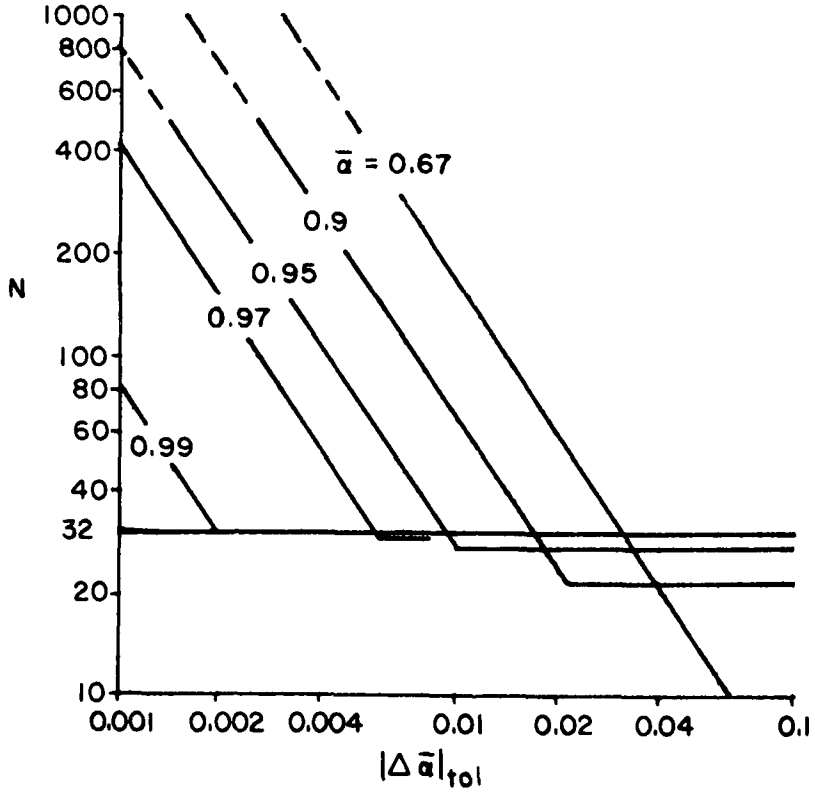

Figure 2. Minimum Number of Particles in an Averaging Volume for given Tolerance $|\Delta\bar{\alpha}|_{tol}$ and k = 0.2

a theory still can be used to represent averages over cross-sectional segments of the gun tube, that is, it can be used to calculate the interior ballistics core flow.

Volume averaging smoothes and distorts not only the undesirable heterogeneities caused by single particles, but also other flow structures, particularly if they have extensions less than a diameter of the averaging volume. An example of a flow structure with a small extension is the boundary of a particle aggregate. Let the average gas volume fraction in the aggregate be $\bar{\alpha}$ and let the aggregate occupy the half-space $z > 0$. Conceptually one thinks of the boundary at $z = 0$ as a narrow transition between a region with $\alpha = 1$ (gas only) and a region with $\alpha = \bar{\alpha}$ (gas particle mixture). The correctly defined α has, instead a finite transition zone between $\alpha = 1$ and $\alpha = \bar{\alpha}$ with a width equal to a diameter of the averaging volume. If the volume is a sphere with the radius R, then the transition is approximately given by the following function (see Appendix D)

$$\alpha(z) = \begin{cases} \alpha = 1 & \text{if } z \leq -R \quad , \\ \alpha = 1 - (1-\bar{\alpha})\,(1+\frac{z}{R})^2\,(2-\frac{z}{R})/4 & \text{if } -R < z < R \quad , \\ \alpha = \bar{\alpha} & \text{if } R \leq z \quad . \end{cases} \tag{2.11}$$

This transition is an idealization, derived under the assumption that the undulations $\Delta\bar{\alpha}$ are zero within the particle aggregate, but it is not the limit curve for $R \to \infty$. (Such a limit is the constant $\alpha = (1+\bar{\alpha})/2$ for any aggregate occupying a half-space). The real transition curve undulates around a basis that is approximated by Eq. (2.11). The amplitude of the undulations is bounded by Eq. (2.3) in which $\bar{\alpha}$ is replaced by the basis value. The approximation (2.11) is quite good even for moderate values of R/L_m, as shown by the examples of transition curves in Section 4.

3. GAS VOLUME FRACTION AS A FUNCTION OF THE AVERAGING VOLUME

We consider the gas volume fraction α in an averaging sphere with the radius R and center coordinate vector $\vec{X}$. We assume that the particles are spheres with radius s and arranged in a regular lattice with a lattice constant L. Let $\bar{\alpha}$ be the limit value of the gas volume fraction for an infinite averaging volume. Then one can define (see Appendix B) a mean distance L_m between particle centers by

$$L_m = 4s(1-\bar{\alpha})^{-1/3} \quad . \tag{3.1}$$

The gas volume fraction depends on the lattice type, the location $\vec{X}$ of the averaging sphere with respect to the lattice, the radius R, the radius s,

and on the lattice constant L. Because α is dimensionless, this dependence can be expressed by a function of the following form

$$\alpha = f_1(\vec{X}/L_m,\ R/L_m,\ s/L_m,\ L/L_m), \tag{3.2}$$

whereby the function f_1 depends on the lattice type. The ratio L/L_m is a constant for a given lattice and, therefore, it can be included in the definition of the function f_1. Also, because of the definition (3.1) the argument s/L_m can be replaced by $\bar{\alpha}$. Hence, one has the following two equivalent representations of the functional dependence of α in a given lattice:

$$\alpha = f_2\ (\vec{X}/L_m,\ R/L_m,\ s/L_m) \tag{3.3}$$

and

$$\alpha = f_3\ (\vec{X}/L_m,\ R/L_m,\ \bar{\alpha}) \quad . \tag{3.4}$$

Eqs. (3.3) and (3.4) show that α is a function of five dimensionless scalar parameters: the three components of the position vector $\vec{X}/L_m$, the averaging radius R/L_m and s/L_m or $\bar{\alpha}$. In this section we investigate the dependence of α on the parameter R/L_m. We may think of this dependence as the result of placing the averaging sphere at a fixed position $\vec{X}/L_m$ within a given lattice and letting its radius R/L_m vary. If R is small, then one obtains either $\alpha = 1$ or $\alpha = 0$, depending whether the fixed center position $\vec{X}/L_m$ is outside or inside a particle. As R/L_m increases, α approaches the value $\bar{\alpha}$ regardless of the center location. Figures 3 through 7 show typical curves of the function $\alpha(R/L_m)$ for four different lattices. (The lattices are defined in Appendix A and α was calculated with the algorithm described in Appendix C).

Figure 3 illustrates the dependence of α on R/L_m in a square cylinder lattice with $\bar{\alpha} = 0.5$. The central graph shows two curves. One curve corresponds to the center location coordinates $\vec{X}/L_m = (0,0,0)$ and starts with $\alpha=0$, because the point of origin is a lattice point and occupied by a solid sphere. The other curve starts with $\alpha = 1$. It corresponds to the center coordinates $\vec{X}/L_m = (0.4,\ 0.2,\ 0)$, which is a point occupied by gas. The upper graph in Figure 3 shows the same two curves in a larger scale. One sees that the undulations of $\alpha(R/L_m)$ around the limit value $\bar{\alpha}$ have a wave length of about one and an amplitude that seems to decrease proportionally to a power of R/L_m. The lower graph in Figure 3 shows the number N of particles that are inside the averaging sphere also as a

function of R/L_m. The two curves corresponding to the two locations of the averaging sphere are almost identical and both approximate the cubic (see also Eq. (B.6) in Appendix B)

$$N = (2R/L_m)^3 \quad . \tag{3.5}$$

Figures 4 through 7 present the same functions as Figure 3 but for different values of $\bar{\alpha}$ and for different lattices. One notices that the qualitative as well as quantitative behavior of the functions are very similar in all cases.

Our goal is to obtain an estimate for the amplitude of the undulations of α about the limit value $\bar{\alpha}$ as a function of R/L_m. To that end one can determine for a fixed $\bar{\alpha}$ and R/L_m the extreme values of α by treating $\vec{X}/L_m$ as a free parameter vector. (One can envision this as moving the averaging sphere with a fixed radius in an infinite lattice until the two positions are found that correspond to minimum and maximum α.) The calculations were done with a simplex algorithm and some results are shown in Figures 8 through 15. The figures show that there are differences in detail between lattices and between cases with different $\bar{\alpha}$, but the general trend of the undulation amplitude is rather uniform in all cases. This trend is illustrated in Figures 16 and 17. Figure 16 shows in the left hand graph the extreme negative deviations $\alpha-\bar{\alpha}$ from Figure 15 plotted over the corresponding values of R/L_m in log,log-scale. The right hand graph shows a similar plot of the extreme positive deviations. Both graphs of Figure 16 are combined into one graph in Figure 17. It is apparent from these figures that the negative and positive deviations behave similarly and that their amplitudes are in general proportional to $(R/L_m)^{-2}$. Plots of the extreme deviations for other lattices look very much like Figures 16 and 17. A combined plot of deviations in all four lattices for $\bar{\alpha} = 0.5$ is shown in Figure 18 and for $\bar{\alpha} = 0.9$ in Figure 19. The different symbols in these figures indicate different lattices and different signs of the extreme deviations. The dispersion of the plotted points shows that none of the considered lattices consistently produces larger undulations than other lattices, and that neither negative nor positive deviations are consistently larger within the R/L_m range considered. An estimated upper bound of the deviations is shown as a straight line in the log,log-plots. It has the equation

$$|\Delta\bar{\alpha}| = 0.5\ (1-\bar{\alpha})\bar{\alpha}^2(R/L_m)^{-2} \quad . \tag{3.6}$$

Eq. (3.6) estimates a bound for the maximum amplitude of undulations for a given size of averaging sphere. Using Eq. (3.5) one can also express the estimate in terms of the number N of particles within the averaging sphere:

(Continued on page 33)

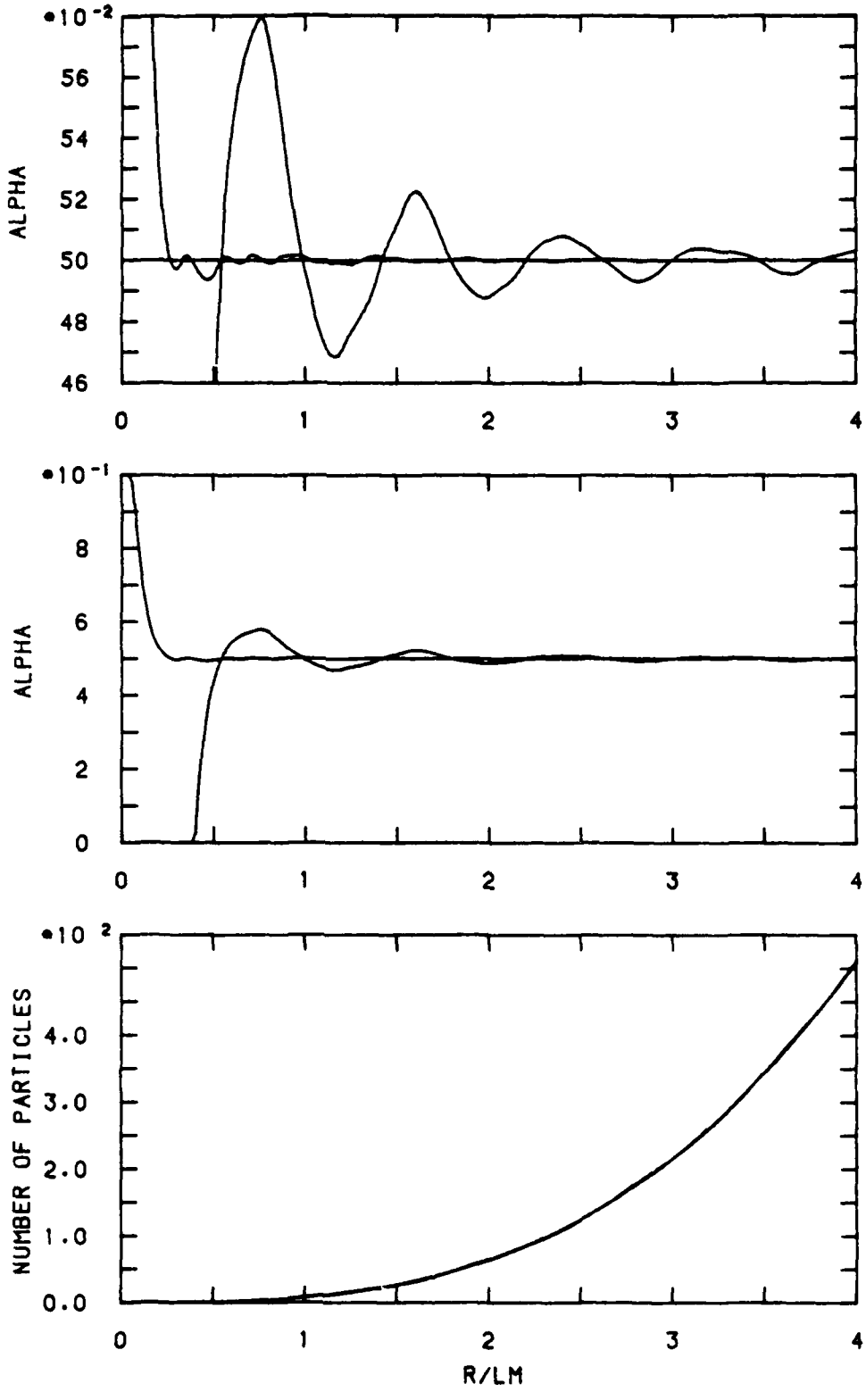

Figure 3. Gas Volume Fraction Dependence on Averaging Radius.

Square Cylinder Lattice, $\bar{\alpha} = 0.5$; $s/L_m = 0.3969$

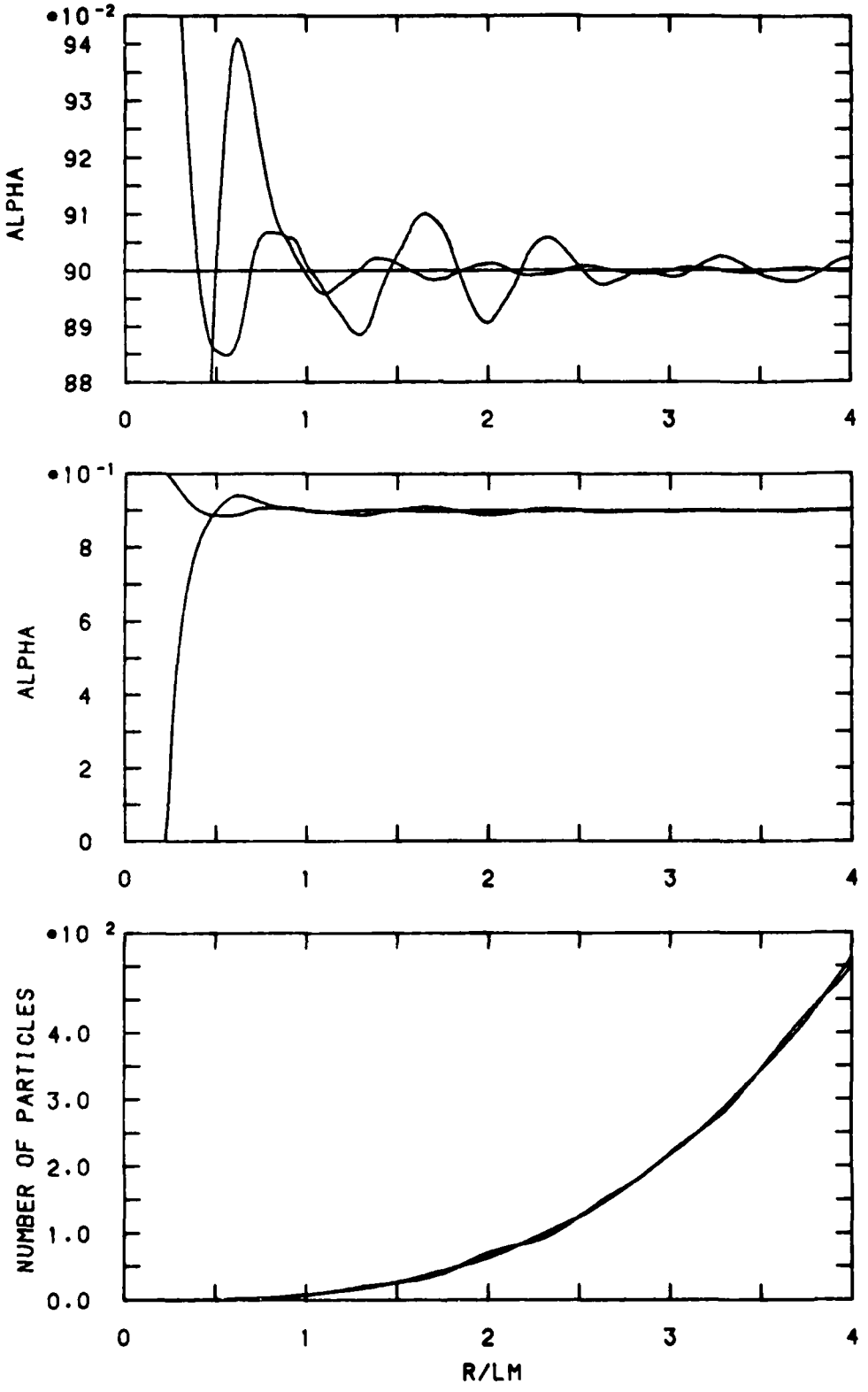

Figure 4. Gas Volume Fraction Dependence on Averaging Radius.

Square Cylinder Lattice, $\bar{\alpha}$ = 0.9; s/L_m = 0.2321

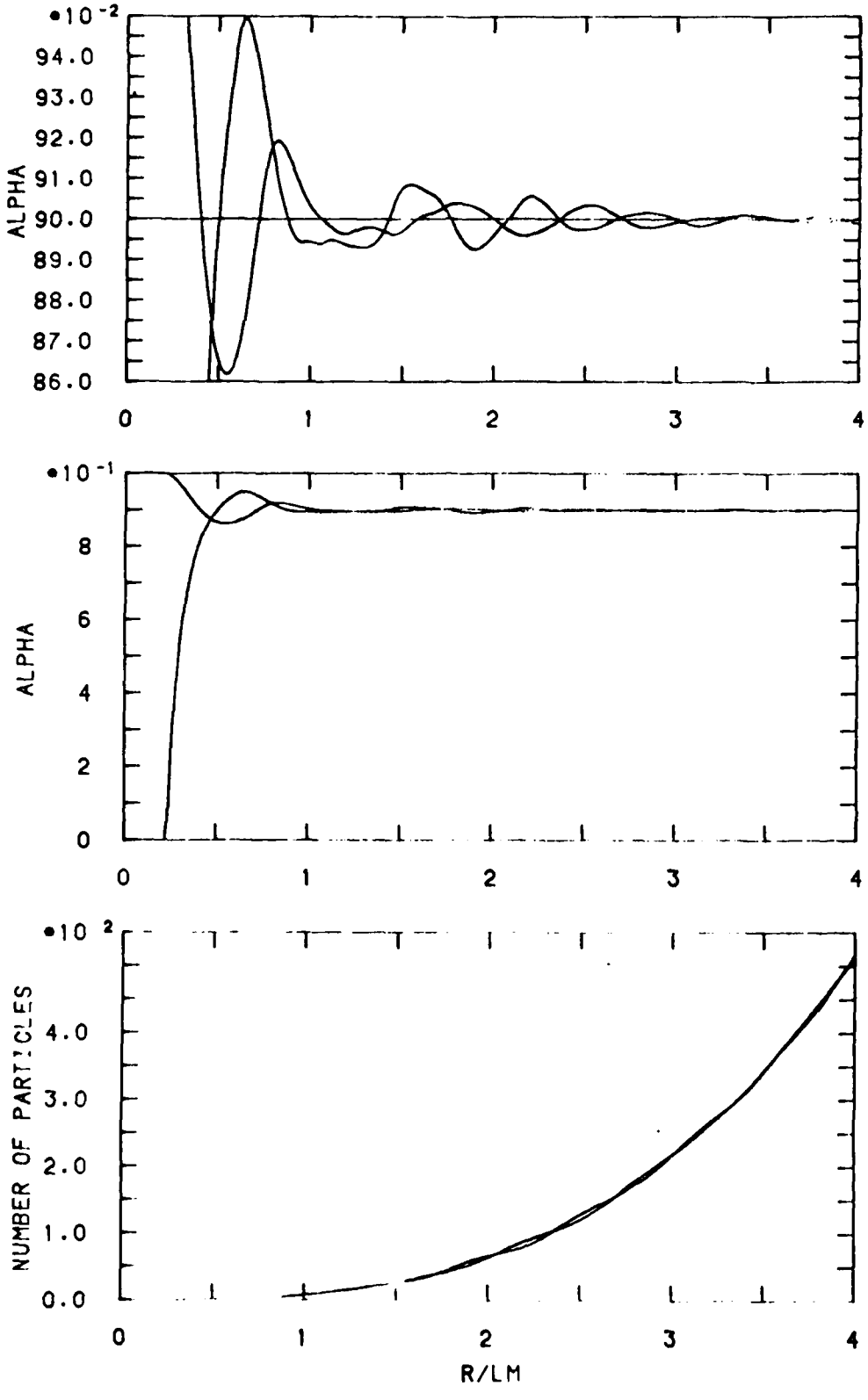

Figure 5. Gas Volume Fraction Dependence on Averaging Radius.

Triangular Cylinder Lattice, $\bar{\alpha}$ = 0.9; s/L_m = 0.2321

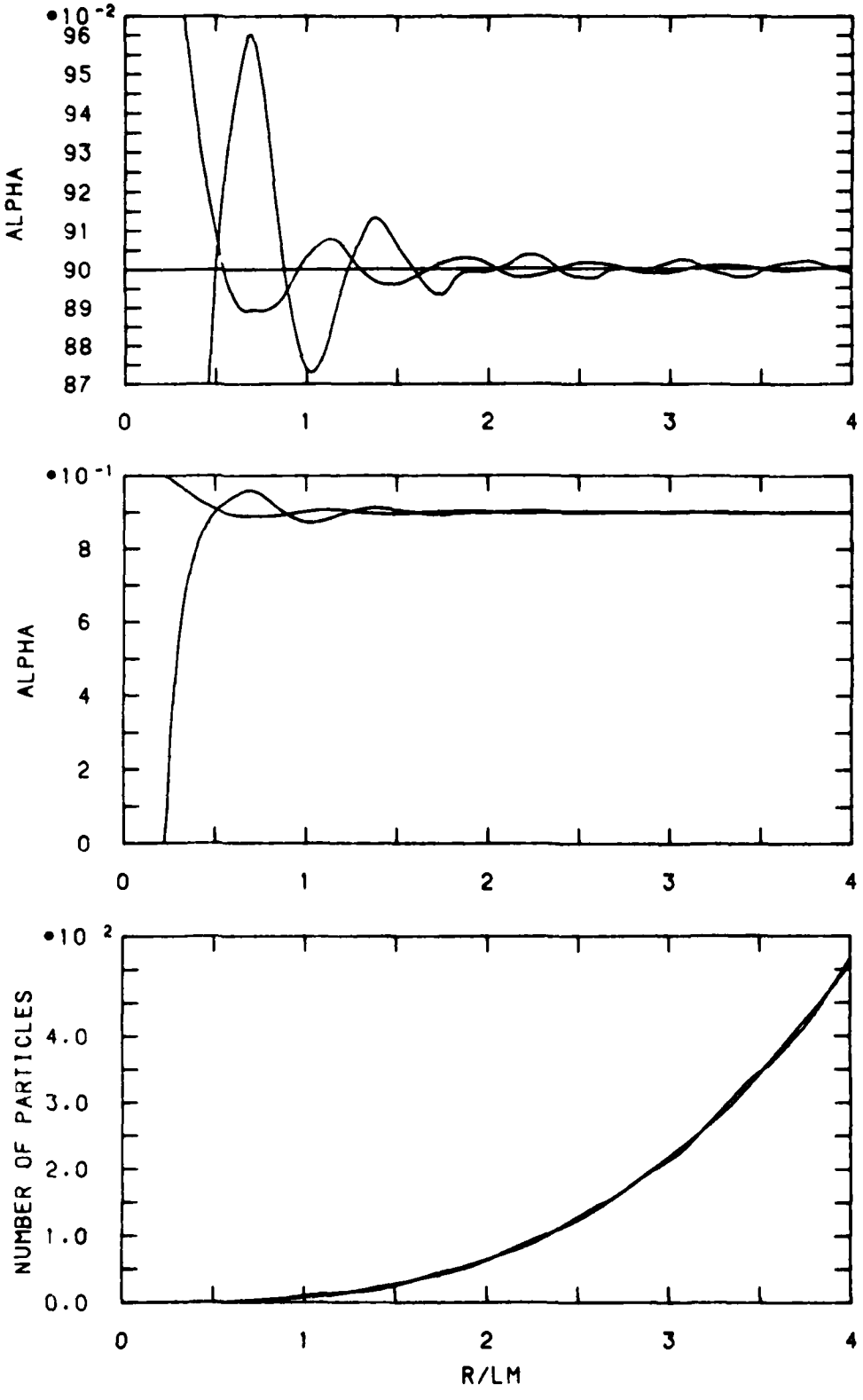

Figure 6. Gas Volume Fraction Dependence on Averaging Radius.

Leap-Frog Square Lattice, $\bar{\alpha} = 0.9$; $s/L_m = 0.2321$

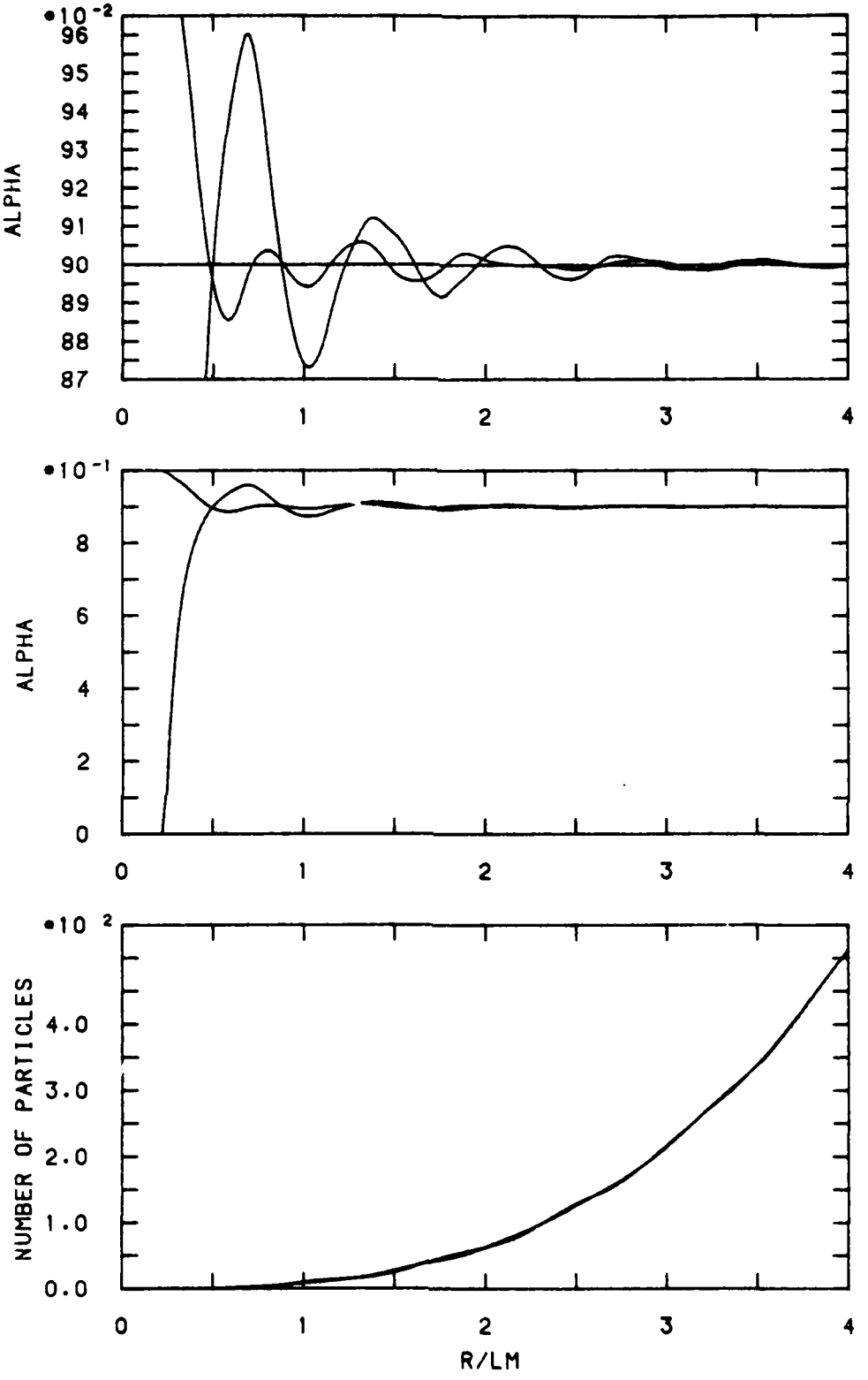

Figure 7. Gas Volume Fraction Dependence on Averaging Radius.

Leap-Frog Triangular Lattice, $\bar{\alpha} = 0.9$; $s/L_m = 0.2321$

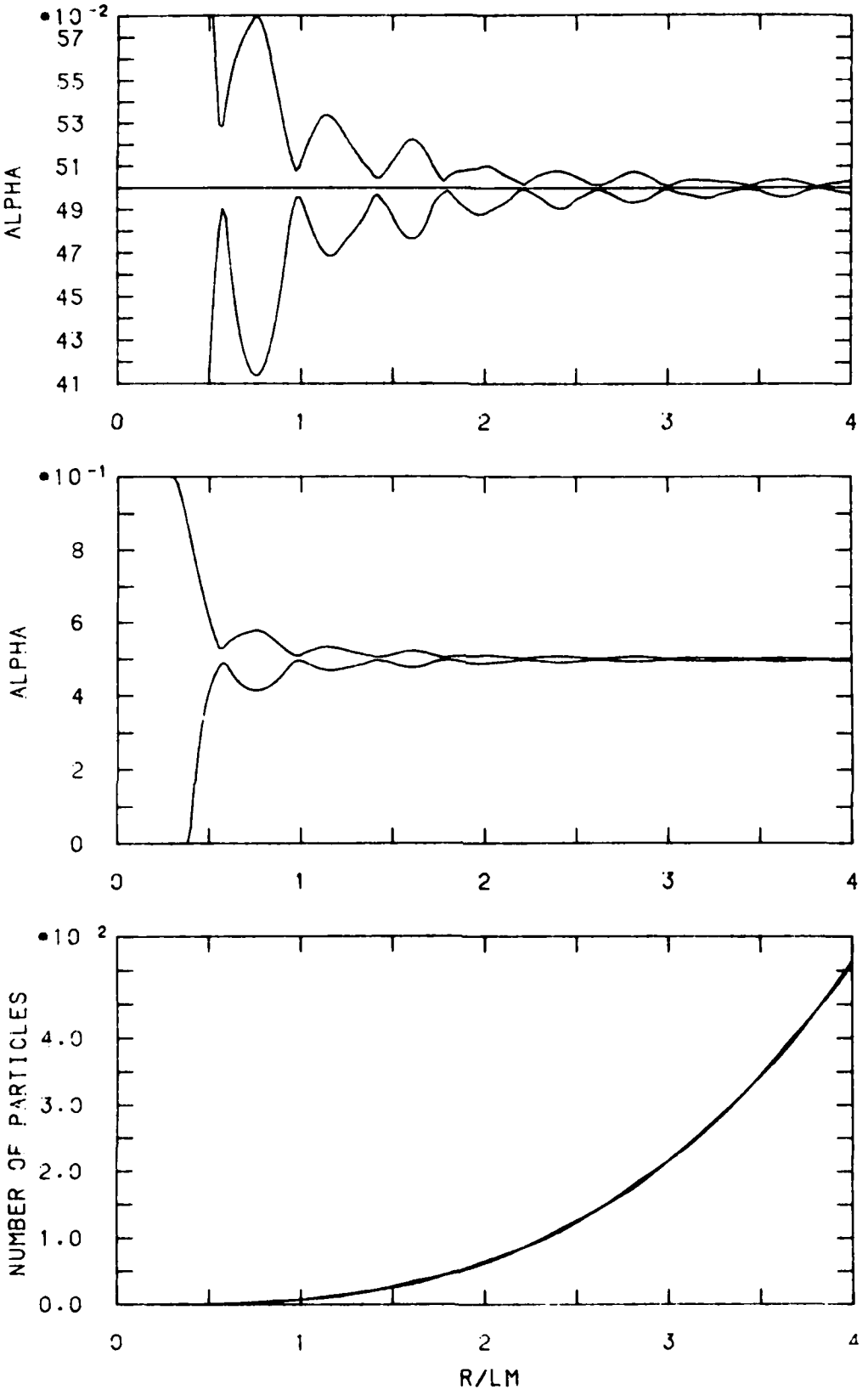

Figure 8. Extremes of Gas Volume Fraction as Functions of Averaging Radius. Square Cylinder Lattice, $\bar{\alpha} = 0.5$; $s/L_m = 0.3969$

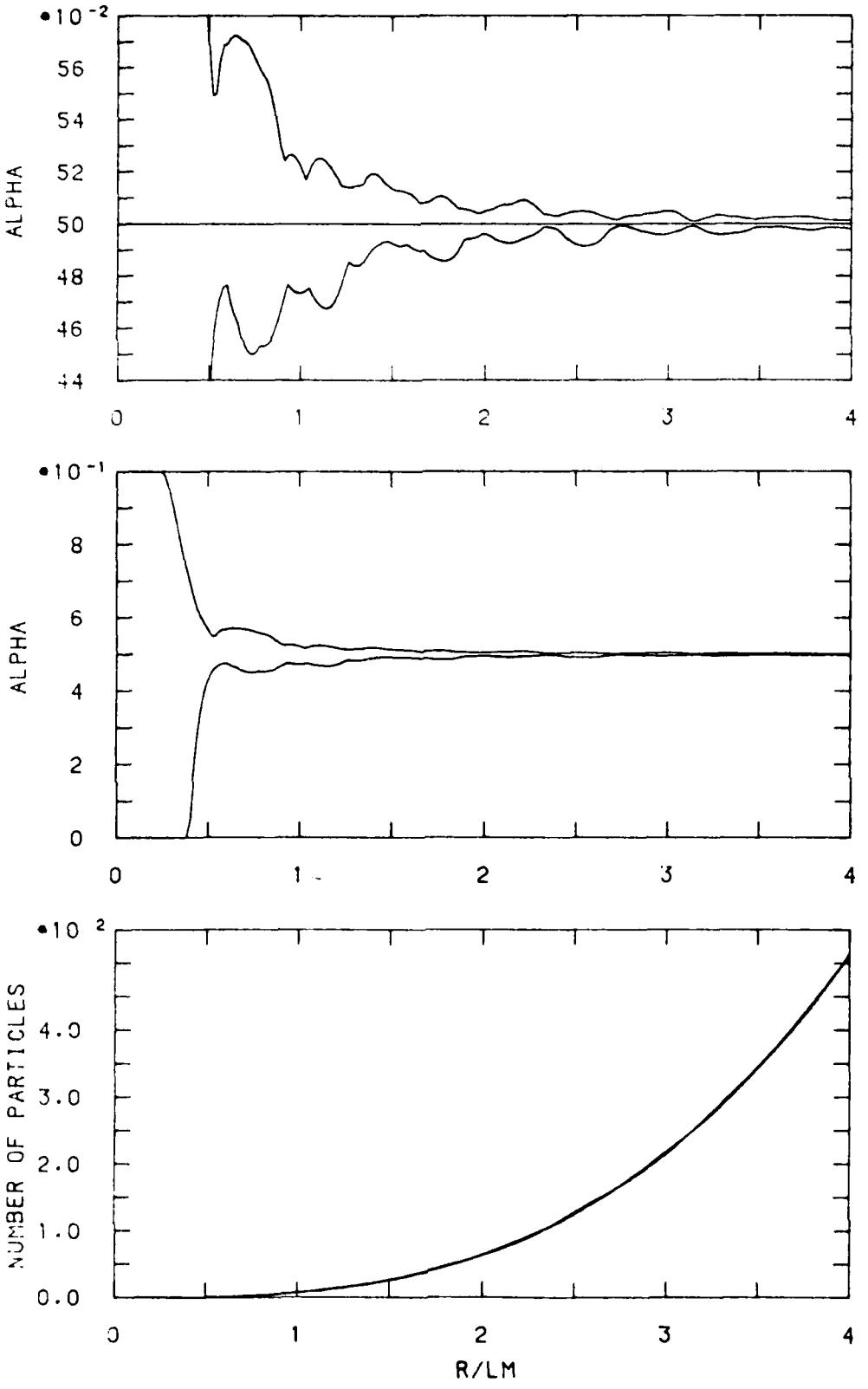

Figure 9. Extremes of Gas Volume Fraction as Functions of Averaging Radius

Triangular Cylinder Lattice, $\bar{\alpha}$ = 0.5; s/L_m = 0.3969

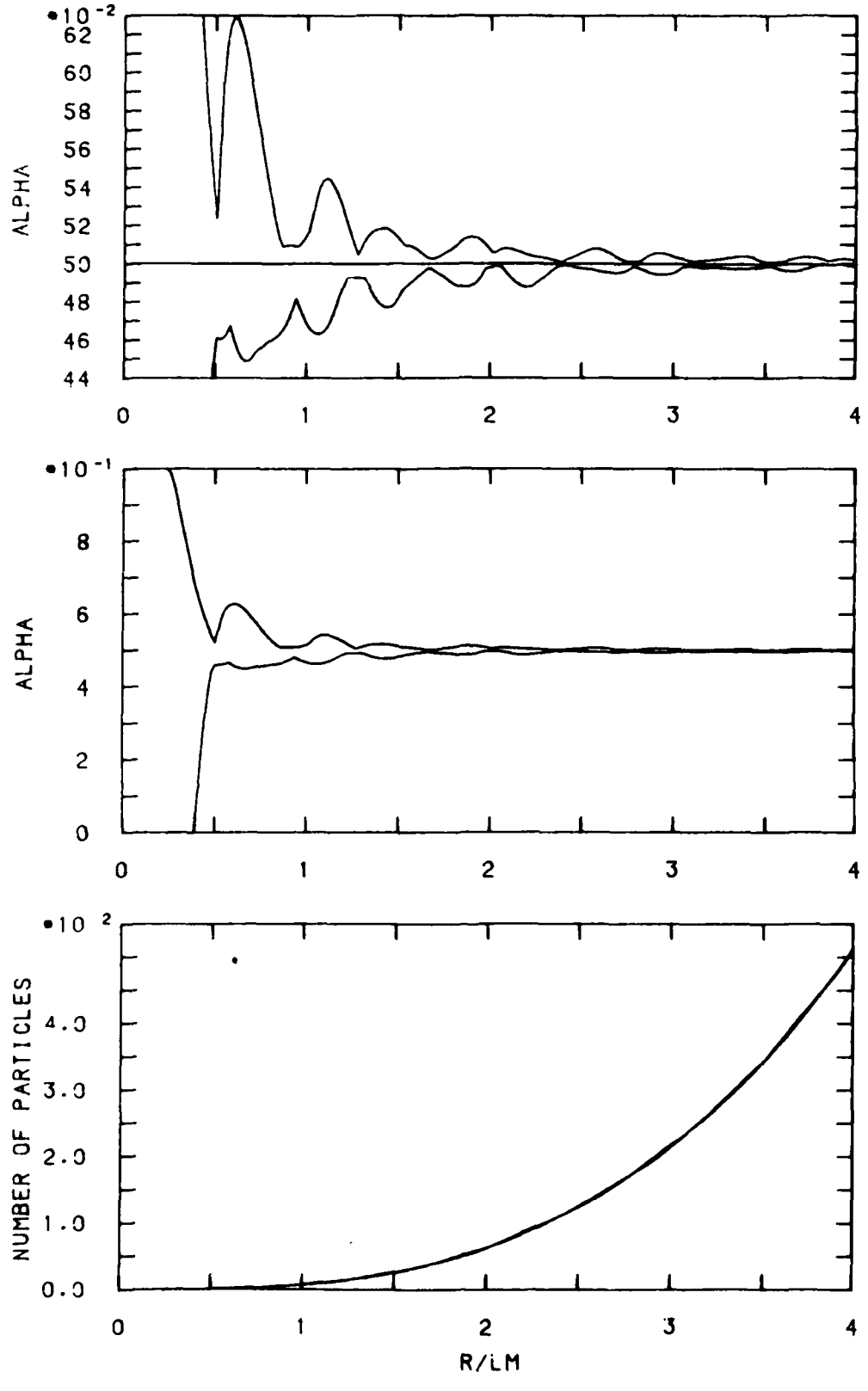

Figure 10. Extremes of Gas Volume Fraction as Functions of Averaging Radius. Leap-Frog Square Lattice, $\bar{\alpha} = 0.5$; $s/L_m = 0.3969$

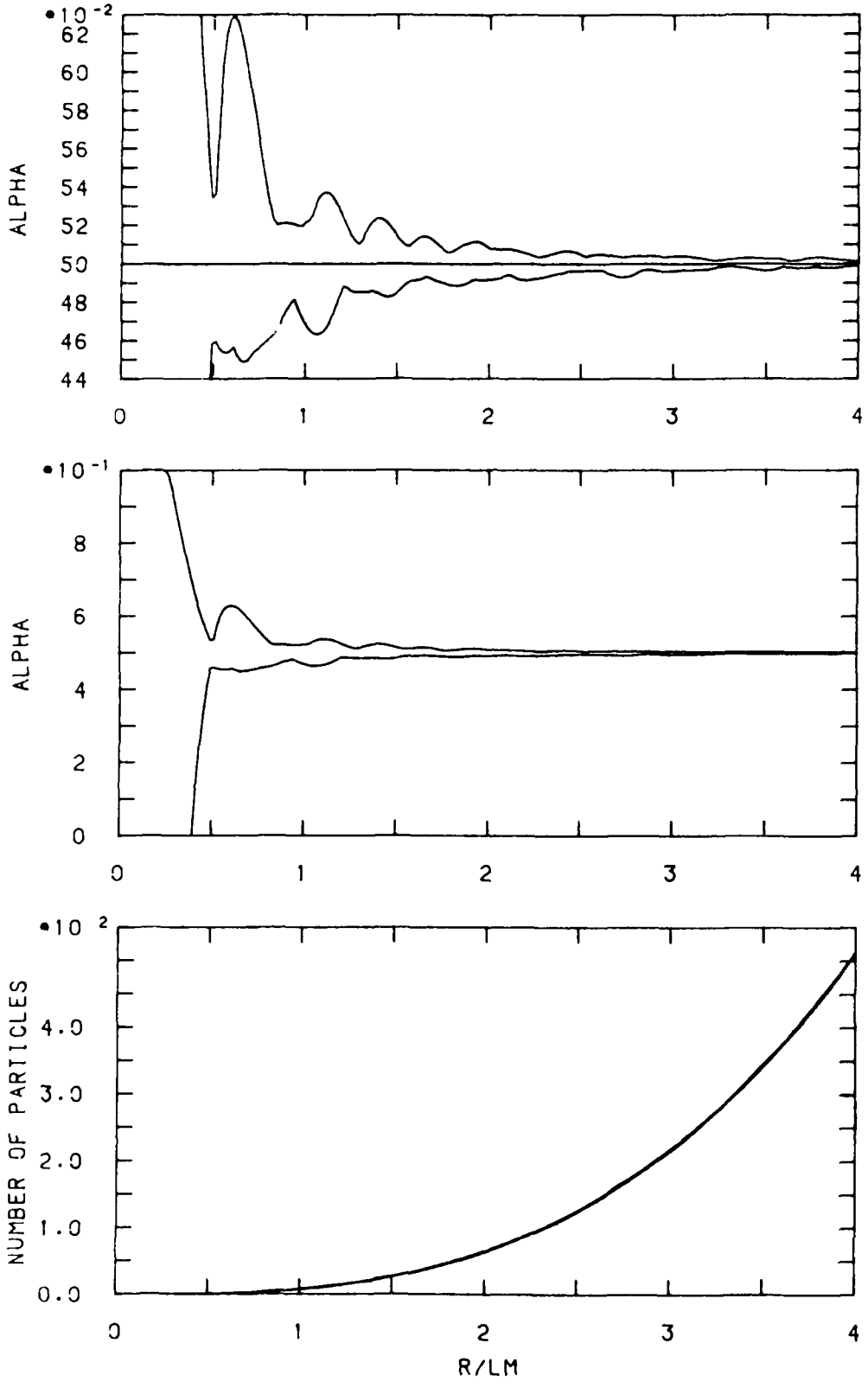

Figure 11. Extremes of Gas Volume Fraction as Functions of Averaging Radius. Leap-Frog Triangular Lattice, $\bar{\alpha} = 0.5$; $s/L_m = 0.3969$

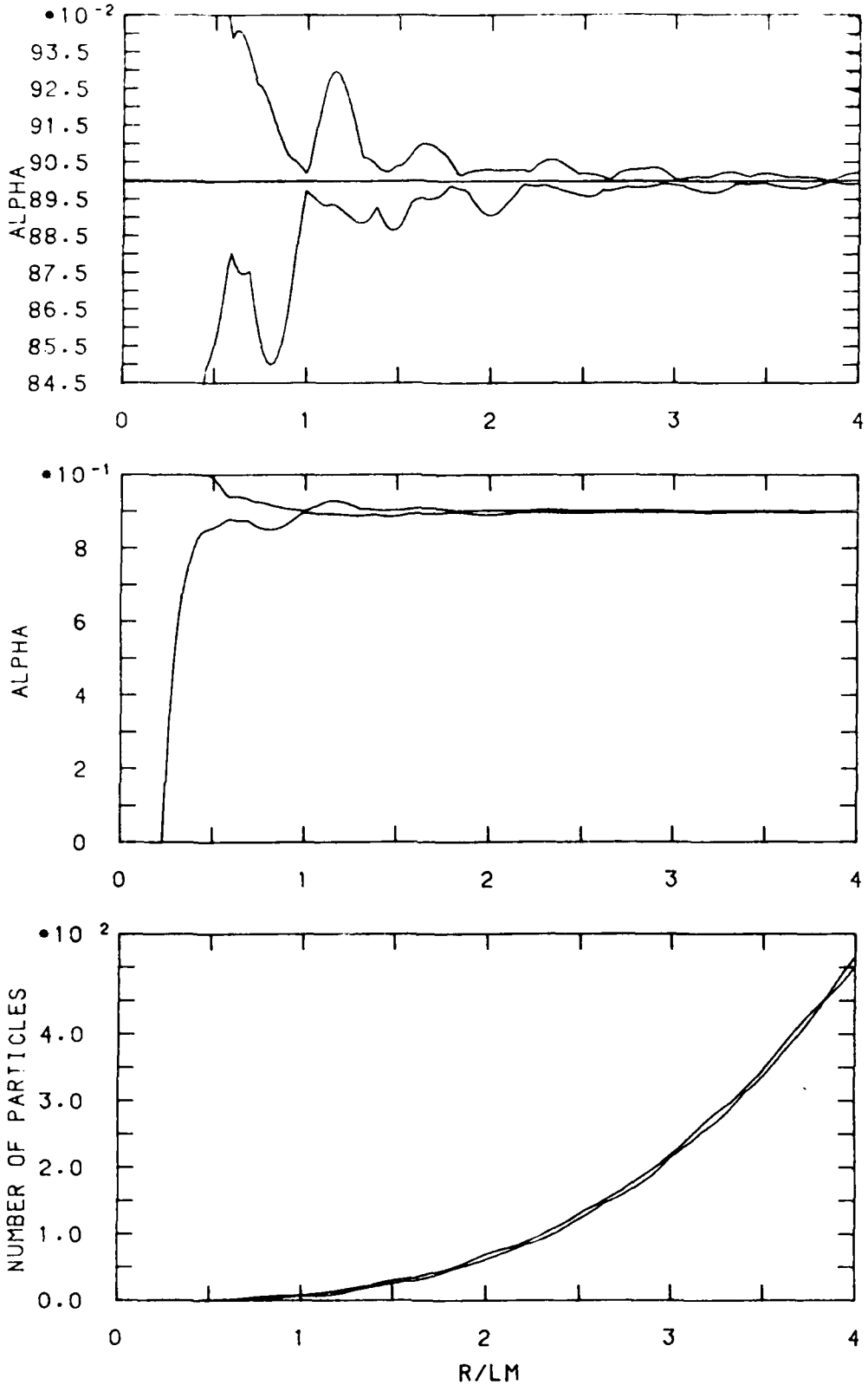

Figure 12. Extremes of Gas Volume Fraction as Functions of Averaging Radius. Square Cylinder Lattice, $\bar{\alpha} = 0.9$; $s/L_m = 0.2321$

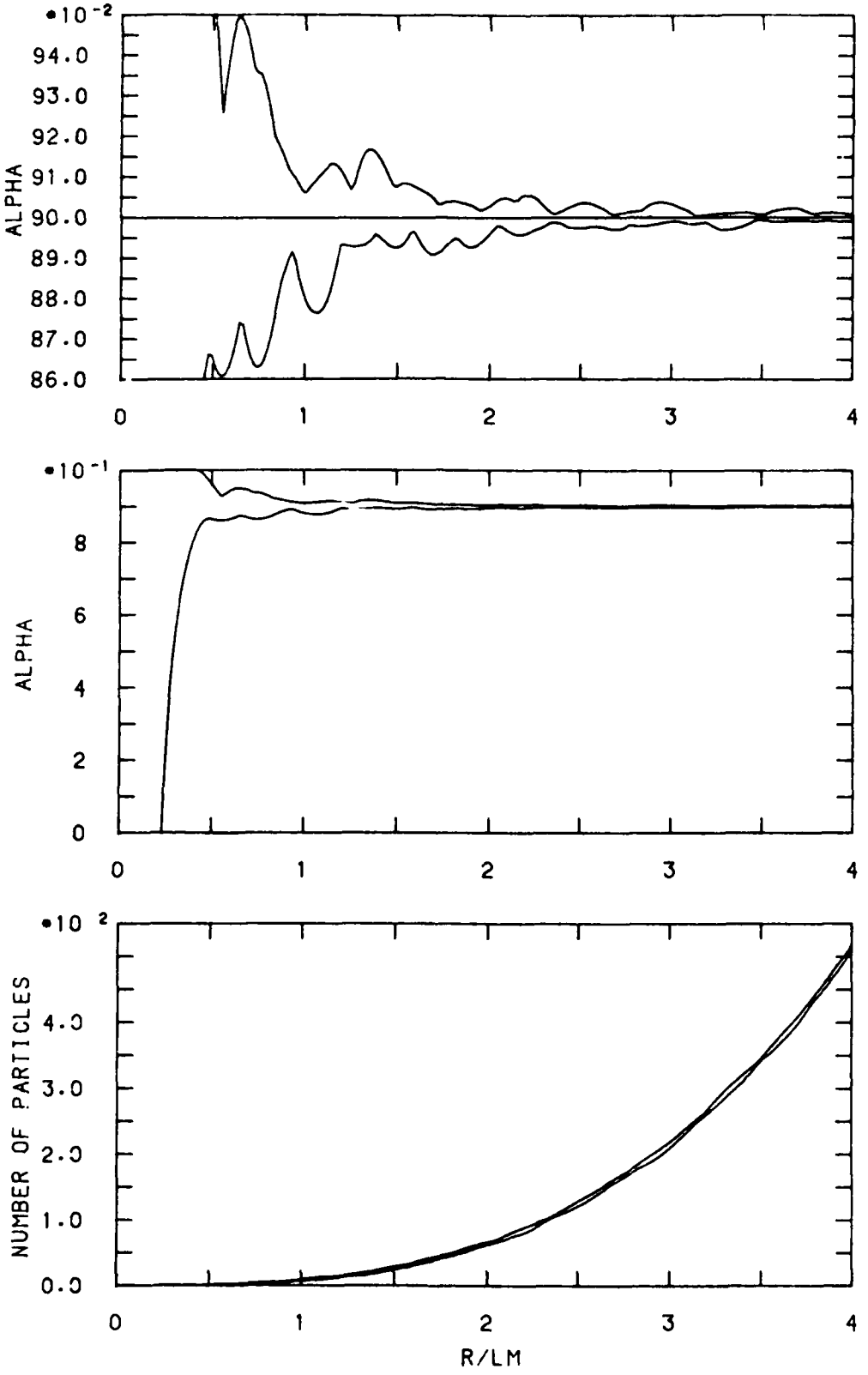

Figure 13. Extremes of Gas Volume Fraction as Functions of Averaging Radius. Triangular Cylinder Lattice, $\bar{\alpha} = 0.9$; $s/L_m = 0.2321$

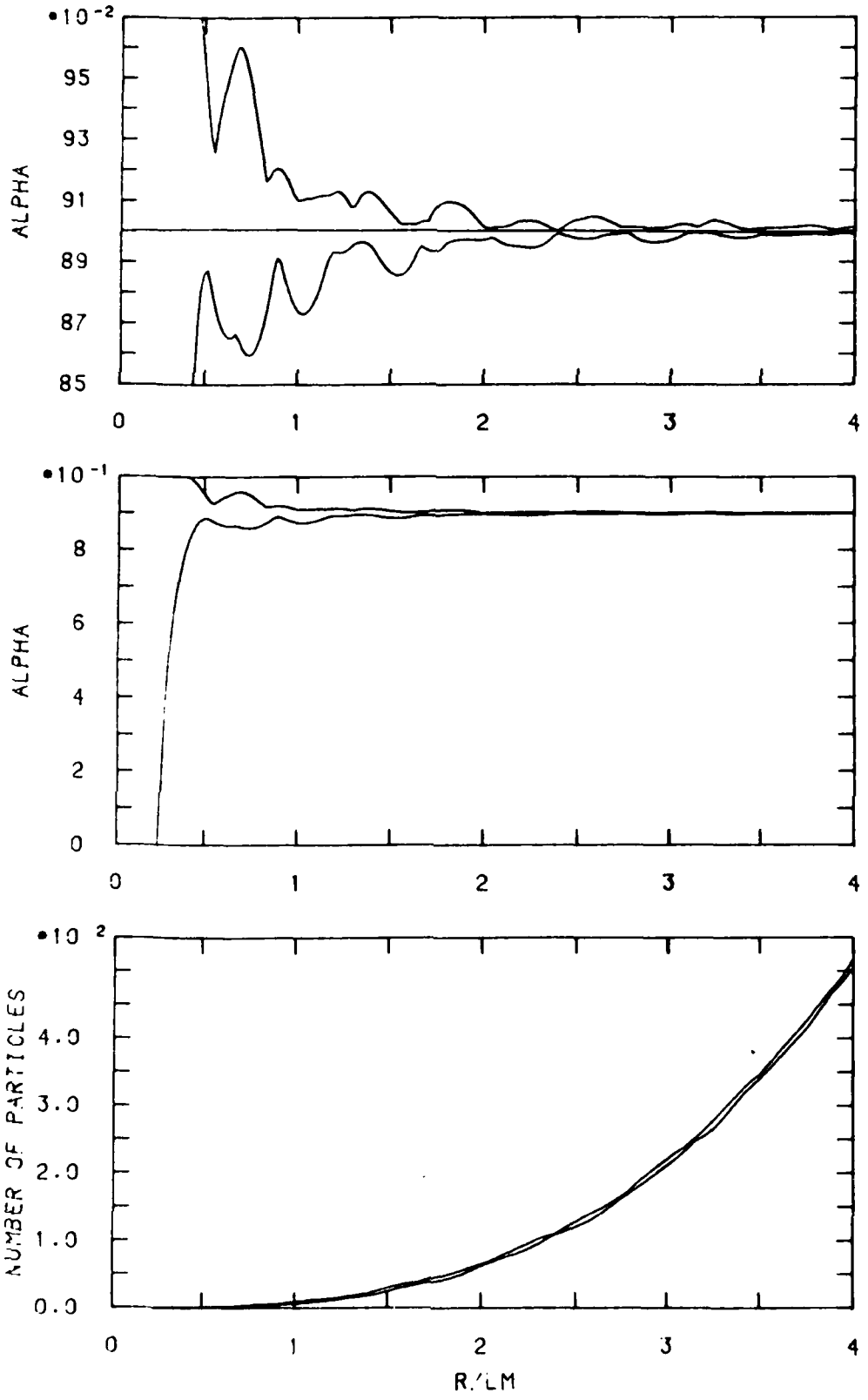

Figure 14. Extremes of Gas Volume Fraction as Functions of Averaging Radius. Leap-Frog Square Lattice, $\bar{\alpha} = 0.9$; $s/L_m = 0.2321$

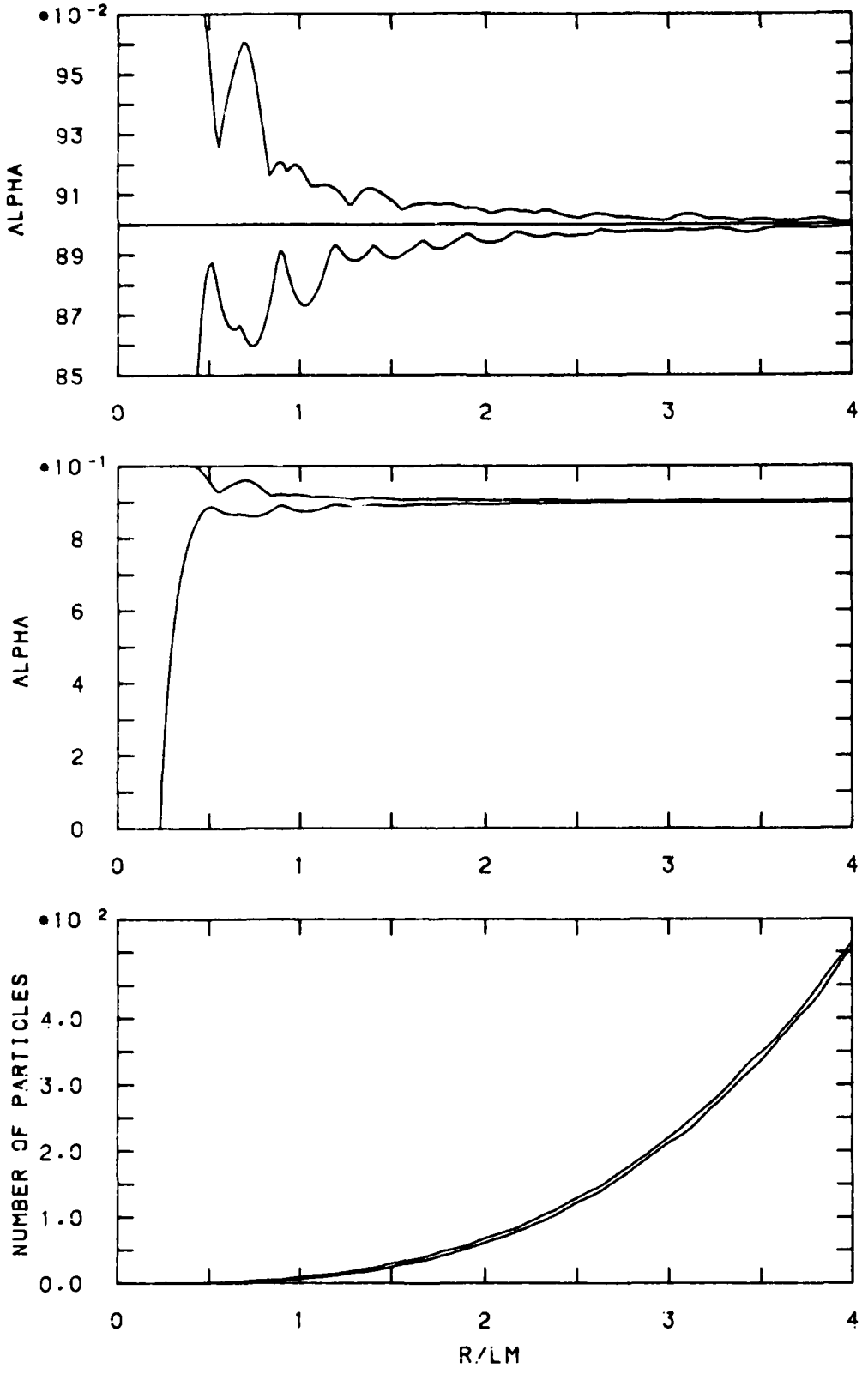

Figure 15. Extremes of Gas Volume Fraction as Functions of Averaging Radius. Leap-Frog Triangular Lattice, $\bar{\alpha} = 0.9$; $s/L_m = 0.2321$

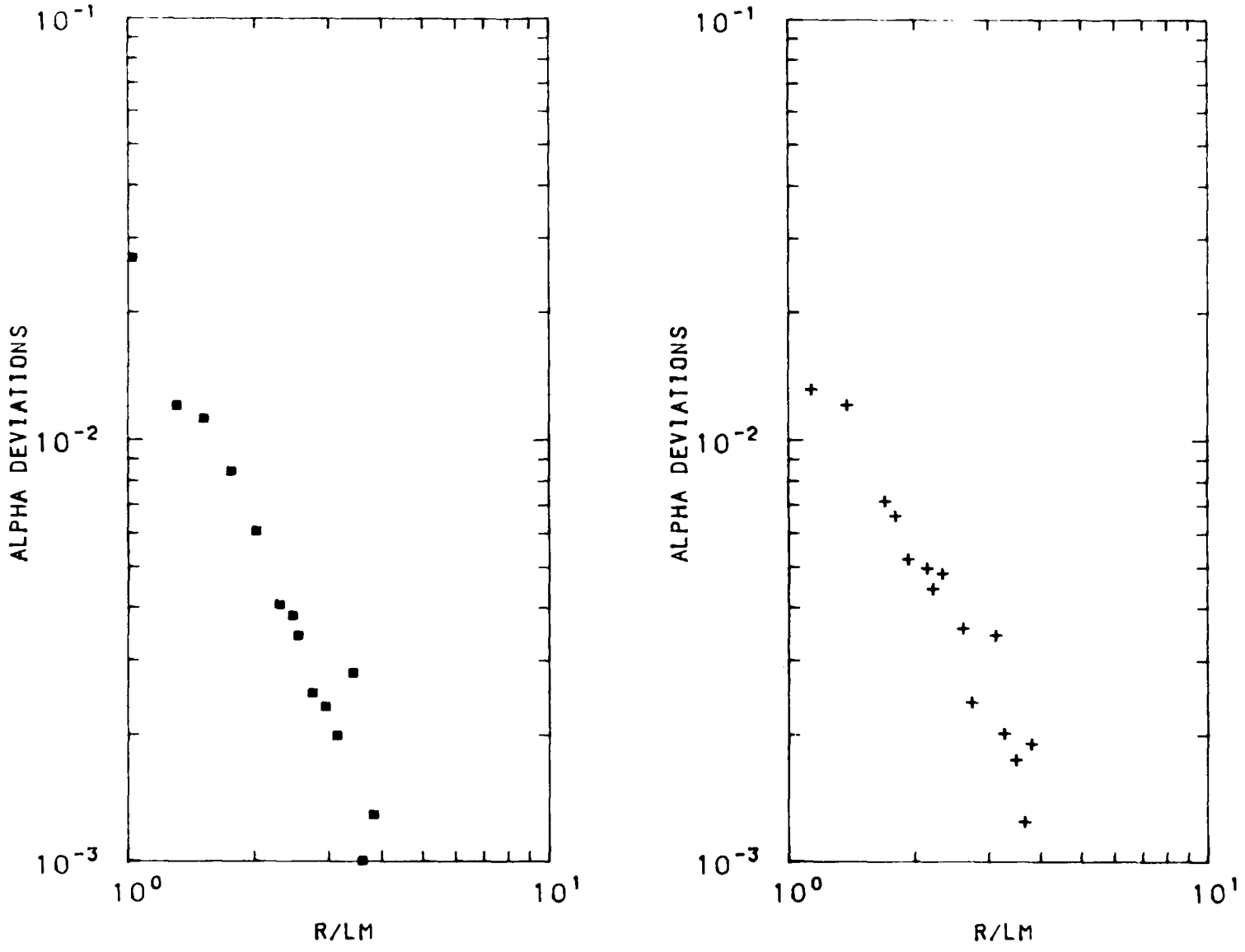

Figure 16. Extreme Deviations of Gas Values Fraction

Leap-Frog Triangular Lattice, $\bar{\alpha} = 0.9$; $s/L_m = 0.2321$

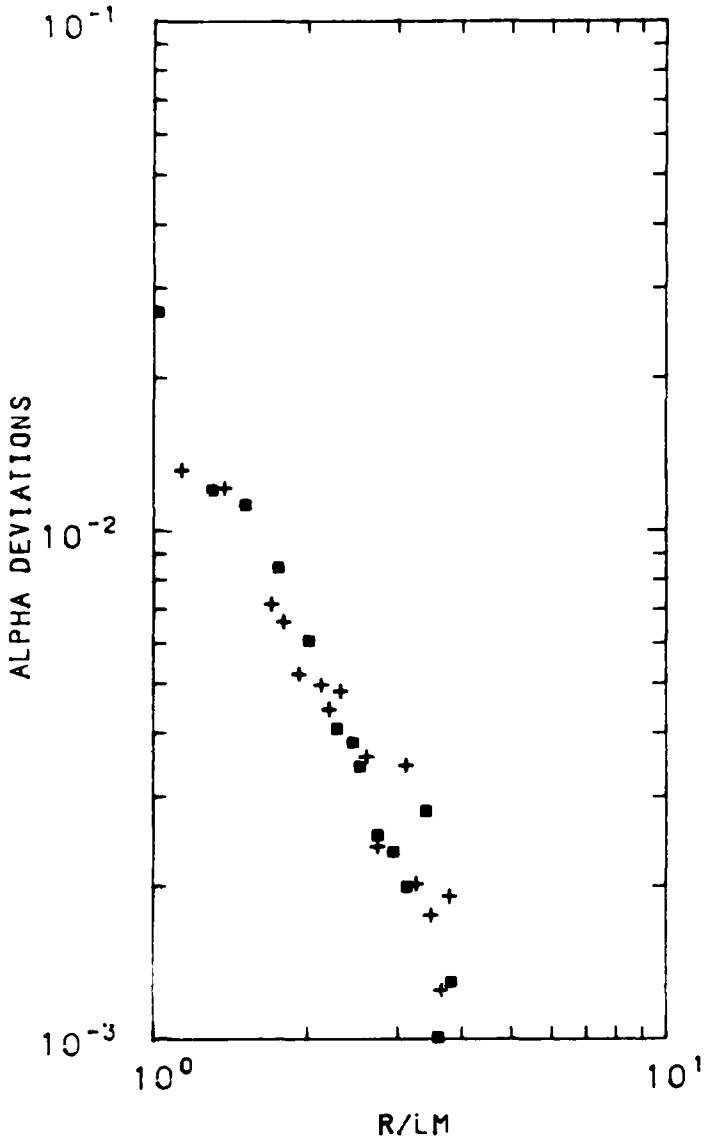

Figure 17. Extreme Deviations of Gas Volume Fraction.

Leap-Frog Triangular Lattice,
$\alpha = 0.9$; $s/L_m = 0.2321$

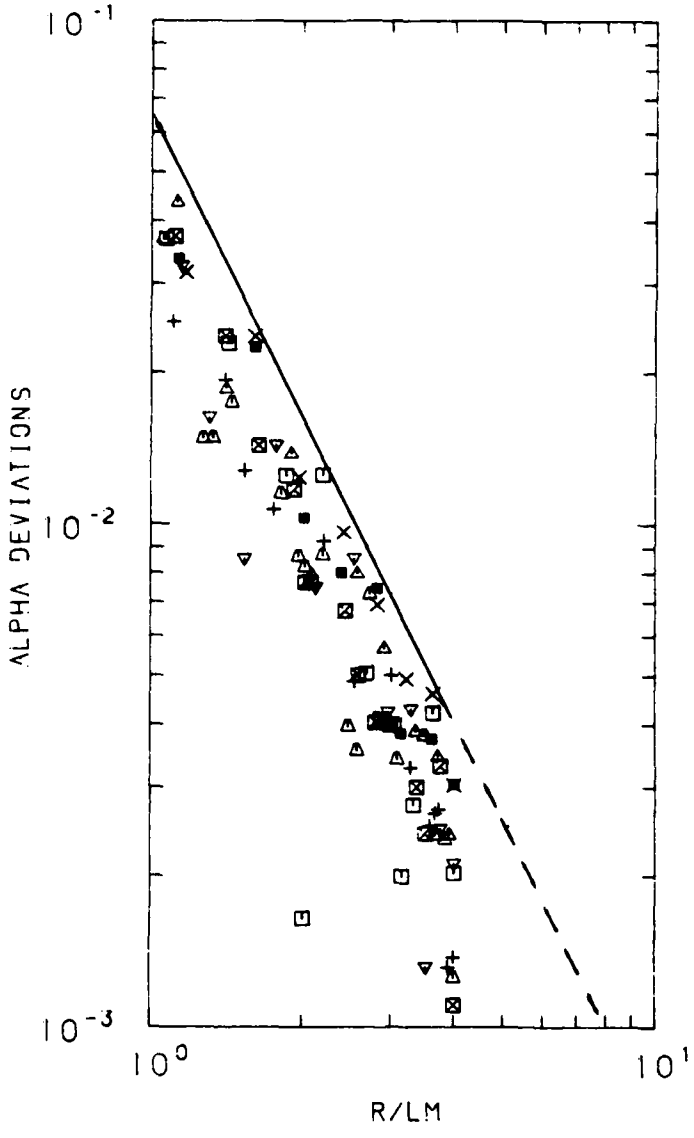

Figure 18. Extreme Deviations of Gas Volume Fraction for All Lattices.

$\bar{\alpha} = 0.5$; $s/L_m = 0.3969$

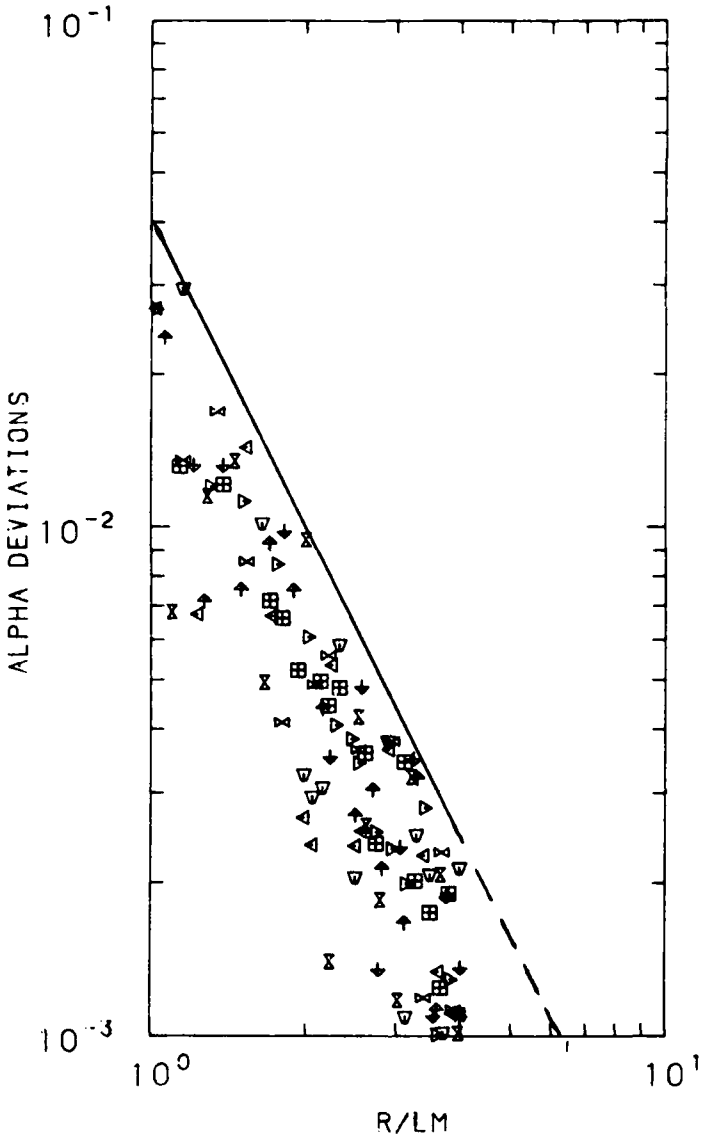

Figure 19. Extreme Deviation of Gas Volume Fraction for All Lattices

$\bar{\alpha} = 0.9$; $s/L_m = 0.2321$

(Continued from page 15)

$$\Delta\bar{\alpha} = 2.0\ (-\bar{\alpha})\alpha^{-2}\ N^{-2/3} \quad . \tag{3.7}$$

If one wants the undulations to be below a tolerance level then Eqs. (3.6) and (3.7) can be used to estimate the corresponding minimum size of the averaging sphere and minimum number of particles within the sphere, respectively. A discussion of such estimates and corresponding graphs are presented in Section 2.

Next we discuss the validity of Eq. (3.6) and (3.7). They are based on sample calculations within the range $1.0 \leq R/L^m \leq 4.0$ (or $8 \leq N \leq 512$) for $\bar{\alpha} = 0.5$, 0.667 and 0.9, and for four different lattices. Because the four lattices have quite different symmetries and maximum packing densities, one can assume that the results are representative for all reasonably regular and uniform particle arrangements. One can of course construct periodic particle arrangements for which the undulations are in excess of the estimated limit at some point. However, in order to do so, one would have to stretch the concepts "uniform" and "regular." The calculations cover all $\bar{\alpha}$ values of practical importance, that is, all $\bar{\alpha}$ values over 0.5. (The formulas (3.6) and (3.7) both have the correct limit $\Delta\bar{\alpha} = 0$ for $\bar{\alpha} = 1$.) We notice that the minimum value of $\bar{\alpha}$ (closet packing of spheres) is between 0.26 and 0.48 for the four lattices considered. (See Appendix A.) Therefore, values of $\bar{\alpha}$ below 0.5 are only possible for special arrangements of the particles, and extrapolation of the general formulas to $\bar{\alpha}$ below 0.5, should be done with reservations. The range of the parameter R/L_m between 1.0 and 4.0 was also chosen by practical considerations. For values of R/L_m below one the undulations are large and irregular, indicating that the corresponding average is not a good representation of a particle aggregate. On the other hand, at $R/L_m = 4$ the undulations have an amplitude of the order 10^{-3}, which is sufficient for most applications. Extrapolations of the formulas to larger values of R/L_m likely will give correct estimates, but they have not been tested by sample calculations.

4. GAS VOLUME FRACTION PROFILES

In this section we give an example of gas volume fraction profiles, i.e., of the dependence of the gas volume fraction α on the trajectory of the averaging sphere, and of the smoothing effect of averaging on a flow structure. The example is a particle aggregate with a uniform limit gas volume fraction $\bar{\alpha}$ that occupies the half-space $z > -s$. (By a uniform limit gas volume fraction we mean that the particles are arranged in a regular pattern (lattice) with the limit value $\bar{\alpha}$ for that part of any infinite averaging sphere that is inside the aggregate.) Let the particles be spheres with radius s. We define the boundary of the aggregate as the plane $z = -s$, that is, the tangential plane to the border particles with a zero z-coordinate of their centers. A naive representation of the particle aggregate in terms of α is by the step function

$$\alpha = \begin{cases} 1 & \text{if } z \leq -s \\ \bar{\alpha} & \text{if } z > -s \end{cases} , \qquad (4.1)$$

However, this representation is not correct because the gas volume fraction is only defined in terms of an averaging volume. (The gas volume is by definition an α-fraction of an averaging volume.) The step function (4.1) does not correspond to any finite or infinite averaging volume and, therefore, cannot be a representation of the aggregate boundary. A true representation of the aggregate has to include a size parameter of the averaging volume, in our case the averaging radius R, and one obtains different transition curves between $\alpha = 1$ (outside the aggregate) and $\alpha \approx \bar{\alpha}$ (inside the aggregate) depending on R, on the trajectory of the averaging sphere crossing the boundary, and on the arrangement (lattice) of the particles.

Figure 20 shows examples of transition curves for two different averaging spheres and two trajectories for each sphere. The spheres have the radiuses $R/L_m = 1.0$ and $R/L_m = 2.0$, respectively, and the two trajectories are along the z-axis and along the line $x/L_m = 0.5$, $y/L_m = 0.5$. The particles are spheres with radius s and they are arranged in a leap-frog triangular lattice. (Lattices are defined in Appendix A.) Figure 20 shows the transition curves in two different scales. The general slopes of the transitions are about $(1 - \bar{\alpha})/(2R/L_m)$, but their details depend on the trajectories. Inside the particle aggregate one observes periodic undulations with an approximate wavelength of $1.5\ L_m$ about the limit value $\bar{\alpha}$. The amplitude of the undulations is bounded by Eq. (3.6) and it of course does not decrease as the averaging sphere is moved deeper into the aggregate.

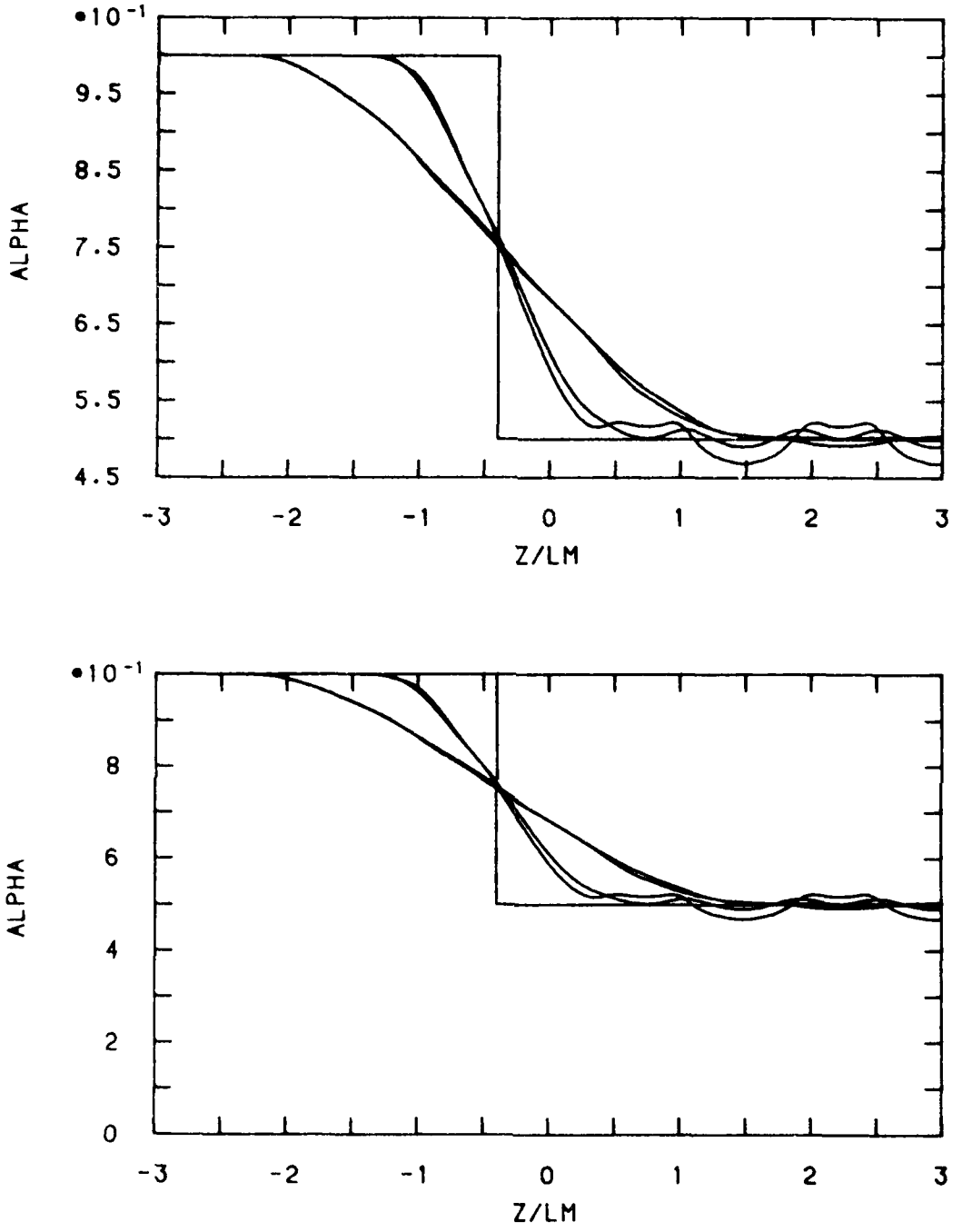

Figure 20. Gas Volume Fraction at a Particle Aggregate Boundary.

$\bar{\alpha}$ = 0.5; s/L_m = 0.3969
R/L_m = 1.0 and 2.0
Leap-Frog Triangular Lattice

Figures 21 and 22 show transitions along the same trajectories and the same lattice, but for other particle sizes, that is, for other limit values $\bar{\alpha}$. The general patterns of the transitions and undulations are the same as in Figure 20, and they are typical for all four lattices considered in this report. The wavelength of the undulations was found to vary between 1.0 L_m and 1.5 L_m, depending on the particle arrangement.

An approximate formula for the transition curve can be derived under the assumption that the undulations within any subsection of the cloud are zero. Then the curve is (see Appendix D)

$$\breve{\alpha}(z) = \begin{cases} 1 & \text{if } z + s \leq -R \\ 1-0.25\ (1-\bar{\alpha})\ [1+(z+s)/R]^2[2-(z+s)/R] & \text{if } -R < z + s < R \\ \bar{\alpha} & \text{if } R \leq z + s \end{cases} \quad (4.2)$$

A representation of the particle aggregate by the function (4.2) is better than Eq. (4.1), because the former takes into account the averaging radius. However, since undulations have been neglected, any real transition curve will deviate from $\breve{\alpha}(z)$ by undulations that are bounded by Eq. (3.6) where $\bar{\alpha}$ is to be replaced by $\breve{\alpha}(z)$. In addition to the undulations, other deviations can be present due to a general structure of the particle arrangement.

The transition curve $\breve{\alpha}(z)$ with bounds computed by Eq. (3.6) and corresponding extreme values of α are shown in Figures 23-25 for a leap-frog triangular lattice. The extreme values were computed for fixed z-values by a simplex algorithm for which the coordinates x and y were treated as free parameters. Conceptually this means moving the averaging sphere within the plane z=const. until the two positions with extreme values of α have been found.

According to Figure 23 the approximation $\breve{\alpha}(z)$ is quite good in this particular case. However, if the particle size is reduced, as in Figure 24, then a systematic deviation becomes apparent in the upper part of the curve. This deviation is also visible in Figure 25, that is, it does not disappear with increased averaging radius. Such deviations were also obtained for other lattices, and they can be positive as well as negative, depending on the lattice and on the orientation of the boundary.

5. DISCUSSION OF THE RESULTS

The sample calculations in Section 3 and 4 show that the gas volume fraction α is a function that undulates about a limit value $\bar{\alpha}$ with a wavelength $1.5 \cdot L_m$ (L_m is a mean distance between particle

(Continued on page 42)

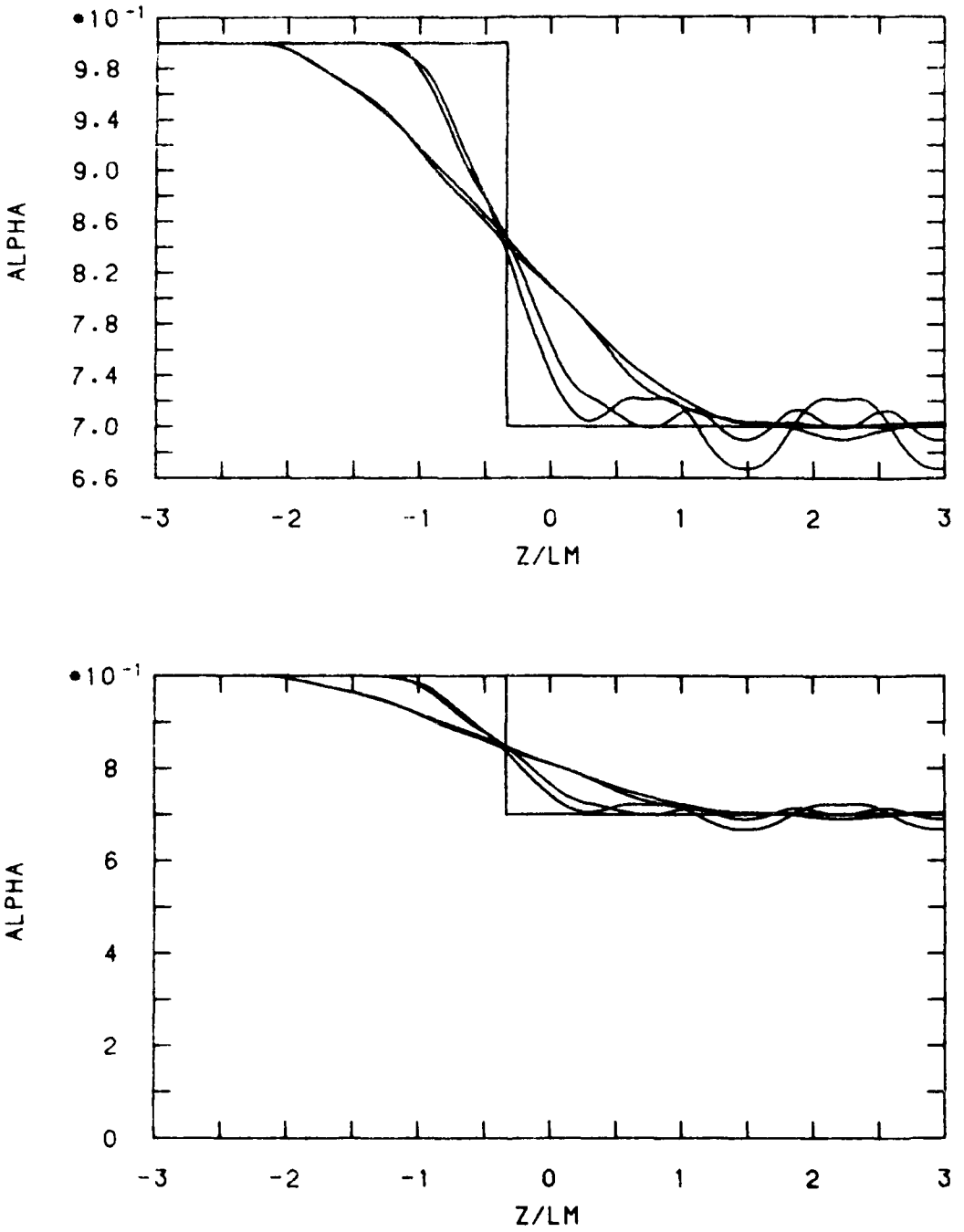

Figure 21. Gas Volume Fraction at a Particle Aggregate Boundary.

$\bar{\alpha}$ = 0.7; s/L_m = 0.3347
R/L_m = 1.0 and 2.0
Leap-Frog Triangular Lattice

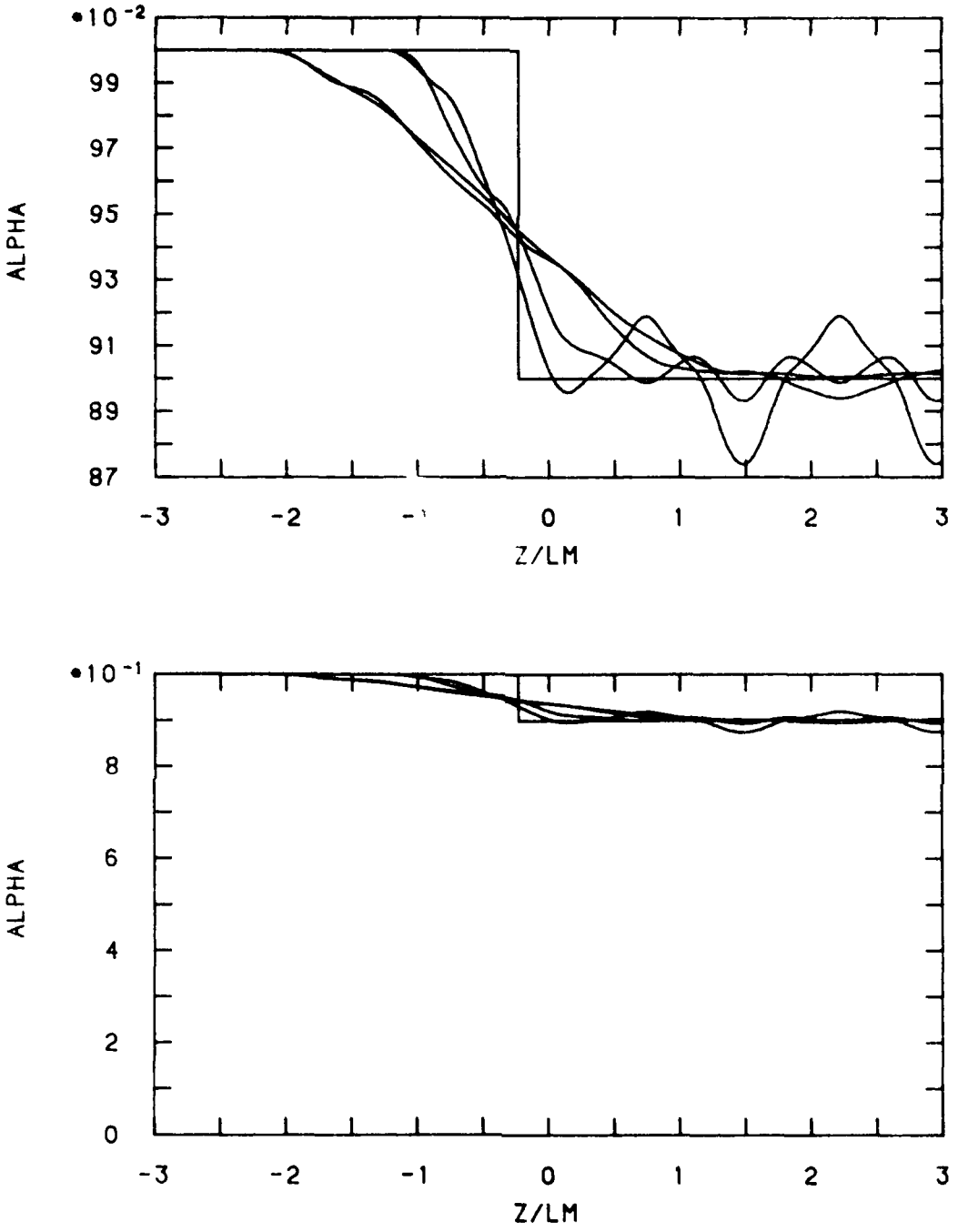

Figure 22. Gas Volume Fraction at a Particle Aggregate Boundary.

$\bar{\tau}$ = 0.9; s/L_m = 0.2321
R/L_m = 1.0 and 2.0
Leap-Frog Triangular Lattice

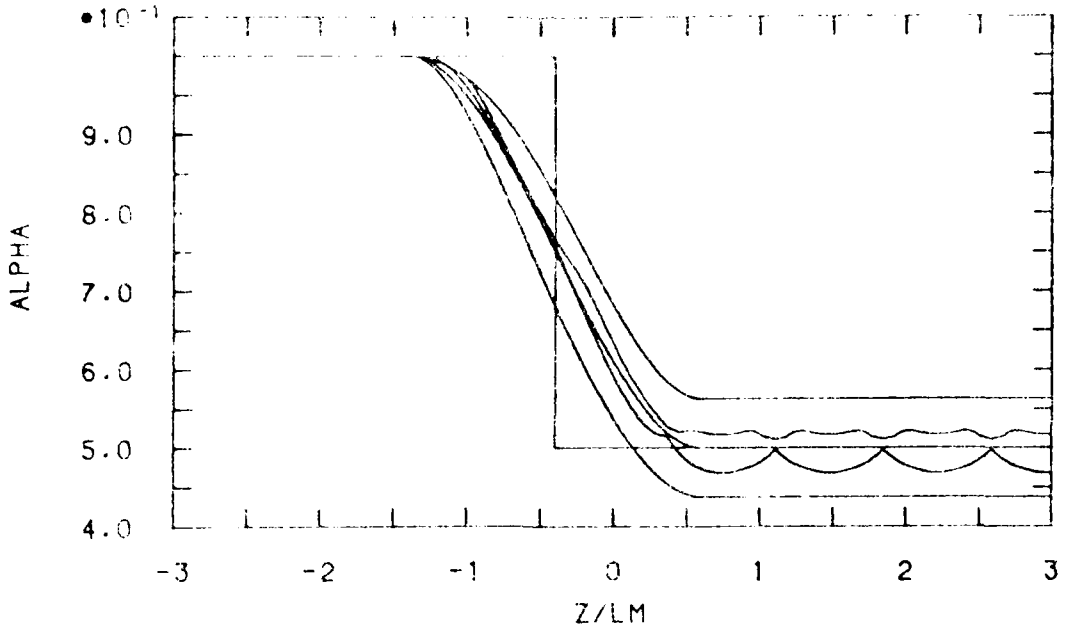

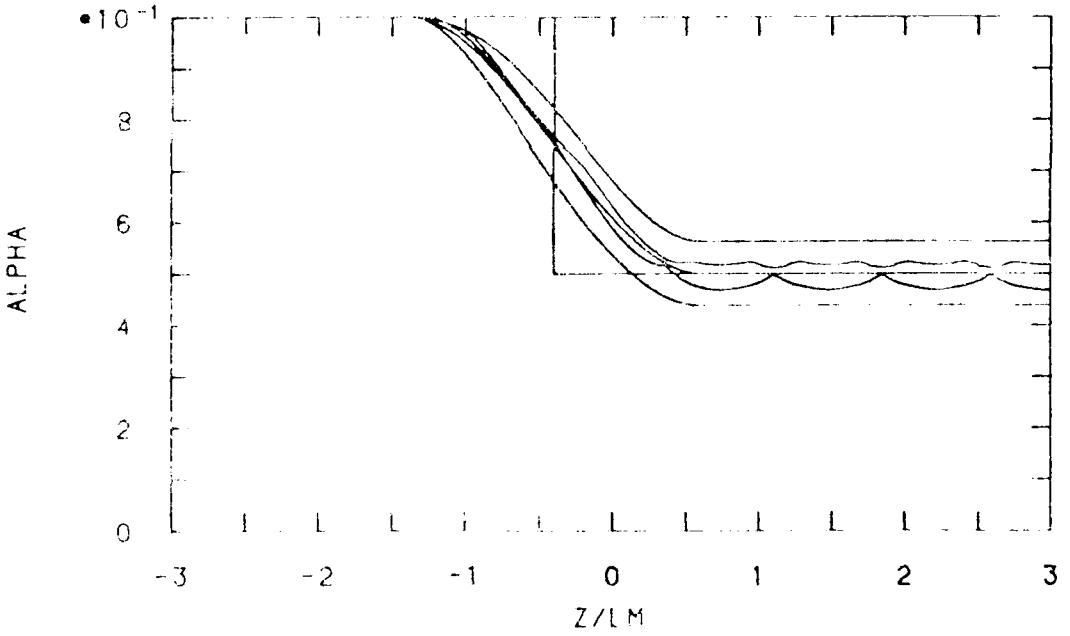

Figure 23. Extreme Values and Estimated Bounds of Gas Volume Fraction at a Particle Aggregate Boundary

$\bar{\alpha} = 0.5$; $s/L_m = 0.3969$
$R/L_m = 1.0$
Leap-Frog Triangular Lattice

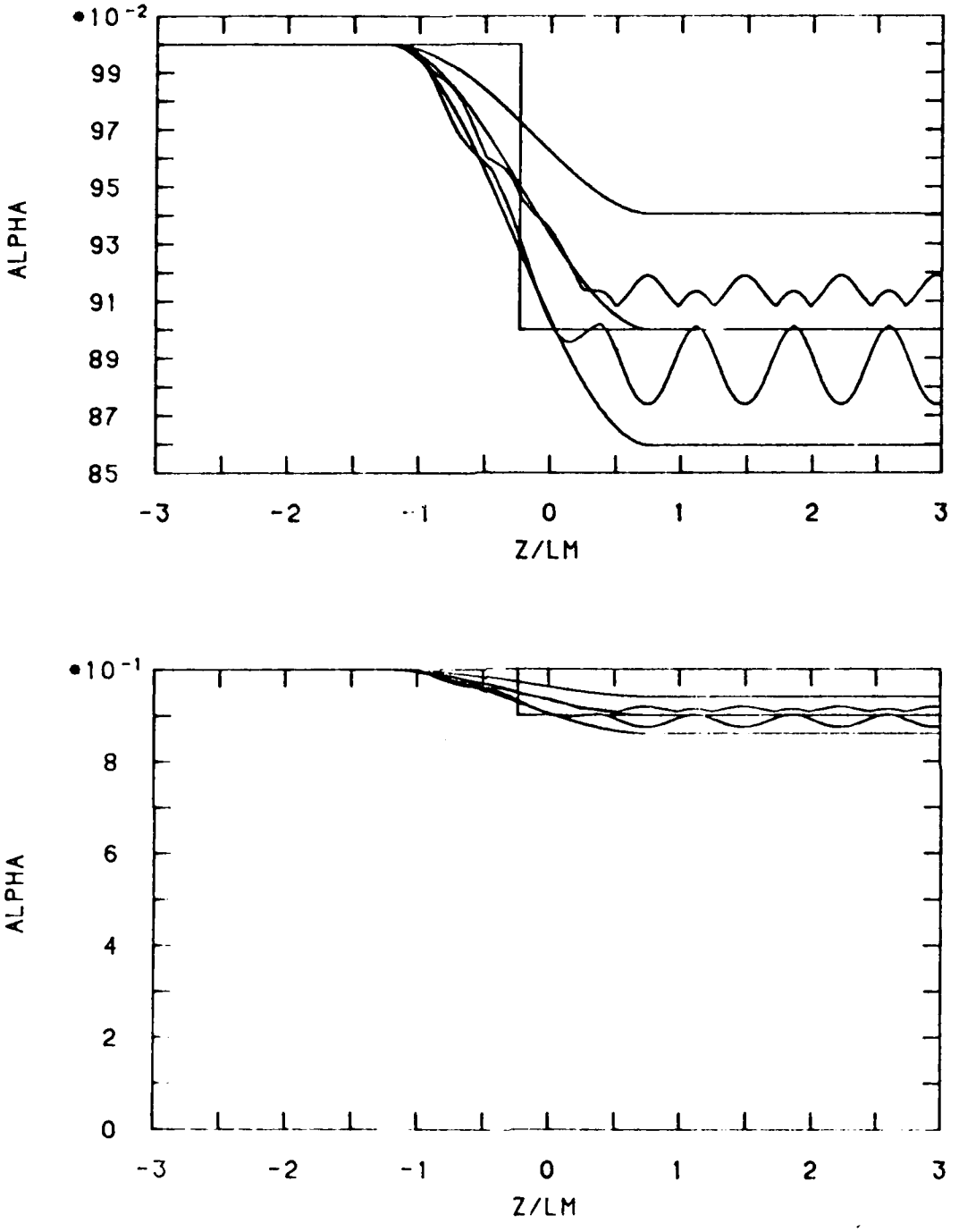

Figure 24. Extreme Values and Estimated Bounds of Gas Volume Fraction at a Particle Aggregate Boundary

$\bar{\alpha} = 0.9$; $s/L_m = 0.2321$
$R/L_m = 1.0$
Leap-Frog Triangular Lattice

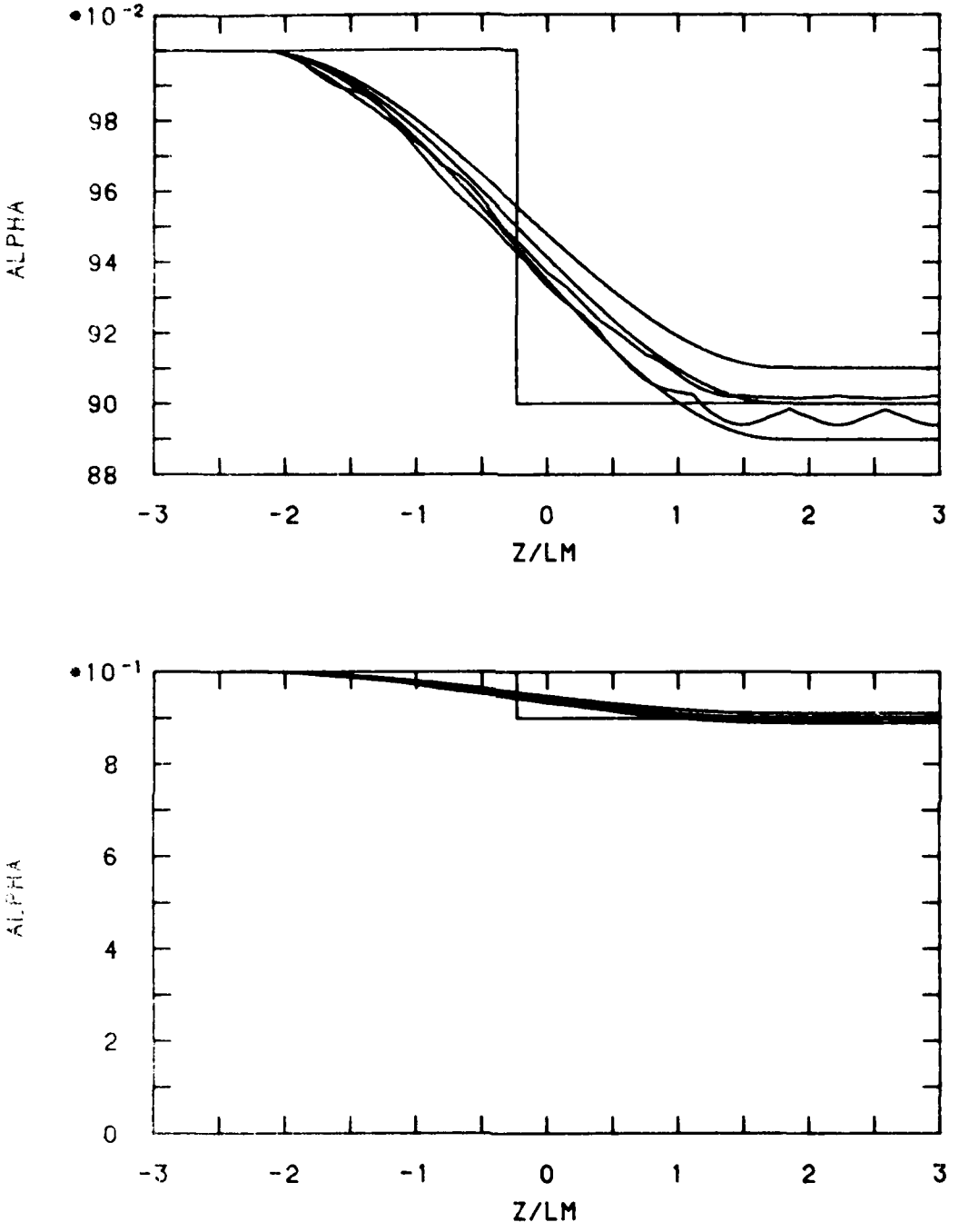

Figure 25. Extreme Values and Estimated Bounds of Gas Volume Fraction at a Particle Aggregate Boundary

$\bar{\alpha} = 0.9$; $s/L_m = 0.2321$
$R/L_m = 2.0$
Leap-Frog Triangular Lattice

(Continued from page 36)

centers) and with an amplitude bounded by Eq. (3.6). Now we discuss consequences of this behavior of α for the representation and computation of a flow field. First, we notice that in an averaged flow field any flow structure with extensions less than R (the radius of the averaging sphere) is smoothed out and also possibly masked by the undulations. Second, the minimum size of R depends on the demands one makes on the averages. Obviously one can only consider an average as a property of a particle aggregate if there are many particles representing the particulate phase within the averaging volume. This remark is quantitated by the estimate of undulation bounds, Eq. (3.6). As the discussion in Section 2 shows, one needs 30-150 particles to keep undulations of α below 0.01 and at least 30 particles if the limit is 0.03. The corresponding minimum values of the radius R are $2.4 \cdot L_m$ and $1.8 \cdot L_m$, respectively. For the sake of the following discussion we assume that R is chosen to be equal to or larger than $2 \cdot L_m$.

The findings have the following consequences for the representation of a two-phase flow field by average flow parameters. Because one cannot distinguish between noise (particle induced undulations) and structures which have extensions less than R, one has to classify as noise any flow structures that extend less than L_m. Consequently, if a flow field is specified in a mesh, the mesh constant need not be finer than L_m. Any mesh refinement can be done by interpolation without loosing accuracy. The same applies to experimental data. If measurements are done locally with a fine mesh then the results should be averaged over a volume corresponding to $R = 2 \cdot L_m$ at least. This applies, of course, also to measurements near boundaries where the averages again represent a finite averaging volume, and not a local point.

Similar consequences can be drawn for the computation of two-phase flow fields, for instance, by solving average flow equations. A reasonable computing mesh constant is of the order of L_m. Refinement of the mesh constant below L_m has at best the effect of interpolation and, at worst, it may induce noise into the solution. In any case such a refinement would waste computing time. If flow structures with extensions less than R appear in the solution, for instance, in mesh refinement studies, then they should be considered as numerical artifacts, because they cannot be interpreted as average flow properties.

These considerations have an interesting result for transient flow fields in which $\alpha \to 1$ in some parts of the field. If α approaches one because the particle sizes are duced (for instance, by combustion) then the condition $R > 2 \cdot L_m$ is not violated and the particulate phase can be represented by averages. If, however, α approaches one because particles diffuse from the mixed phase region into gas-only regions, then the condition $R > 2 \cdot L_m$ will be eventually violated and the average model invalidated. A correct approach in such a situation is to model the rarified parts of the particle aggregate by some other method than averaging, for instance, by individually tracing the diffused particles.

In Appendix B we discuss the value of the mean distance L_m between particle centers and conclude that in typical interior ballistics problems L_m can be as large as three initial propellant particle diameters. According to Figure 1 one then needs an averaging sphere radius that is equal to 6 to 8 initial particle diameters in order to keep the undulations below 0.01. For some interior ballistics situations this means that no flow details in radial direction can be represented by a two-phase theory that is based on averaging, because the minimum diameter of the averaging sphere approaches the diameter of the barrel. In such situations the two-phase theory only can model averages taken over a cross-sectional segment of the barrel, that is, the theory can be used to compute the interior ballistics core flow.

APPENDIX A.

LATTICES

APPENDIX A

LATTICES

For the calculation of the gas volume fraction α one has to specify the size and the spacial arrangement of the particles. In this report, the arrangement is assumed to be in the form of a three-dimensional lattice. In order to assess the significance of the arrangement, four different lattices were used for the calculations. These lattices are defined in this appendix.

The **square cylinder lattice** is shown in Figure A.1. It may be constructed by arranging the particles in a square pattern with a mesh constant L in the x,y-plane, and translating the arrangement in the z-direction by multiples of L. Each original square thereby generates a square cylinder. The lattice is identical to the well-known cubic lattice.

We identify each lattice point by three integer parameters, i,j, and k. The Cartesian coordinates of a lattice point with the identification (i,j,k) are

$$\begin{aligned} x(i,j,k) &= iL \quad , \\ y(i,j,k) &= jL \quad , \\ z(i,j,k) &= kL \quad . \end{aligned} \tag{A.1}$$

The centers of the particles are assumed to be located at the lattice points. Let s be the radius of a particle. If the square cylinder lattice occupies an infinite space, then the corresponding gas volume fraction is

$$\bar{\alpha} = 1 - \frac{4}{3}\pi \left(\frac{s}{L}\right)^3 \quad . \tag{A.2}$$

The smallest value of $\bar{\alpha}$ is obtained if the particles are as large as possible. Because s cannot be larger than L/2 without intersection between particles, one obtains from Eq. (A.2)

$$\bar{\alpha}_{min} = 1 - \pi/6 = 0.476\ 401\ 2 \quad . \tag{A.3}$$

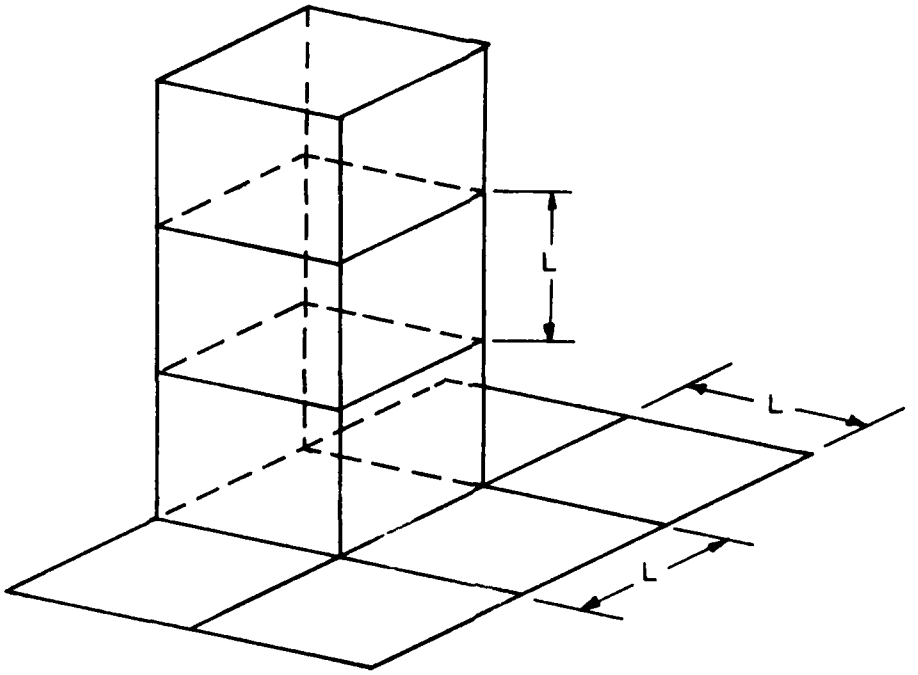

Figure A.1. Square Cylinder Lattice

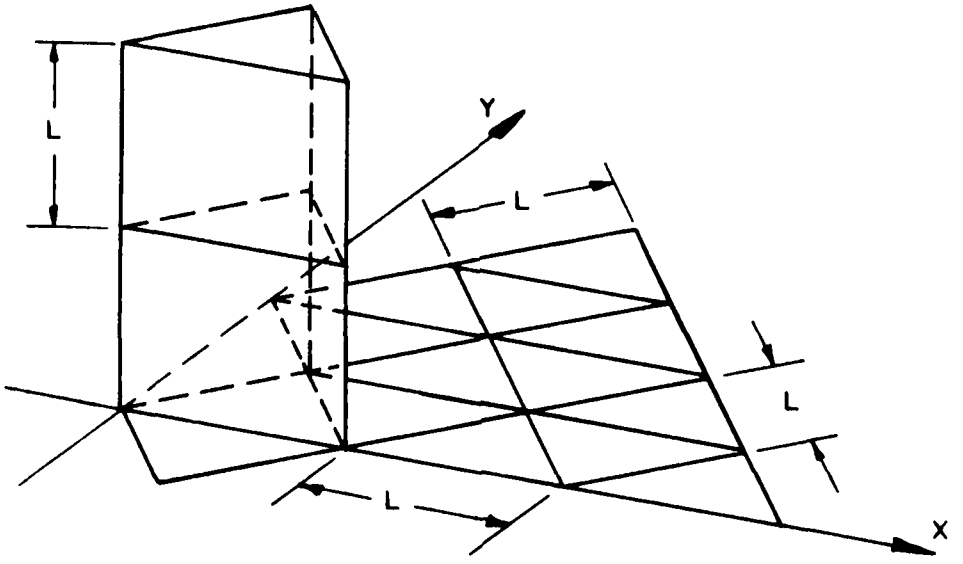

Figure A.2. Triangular Cylinder Lattice

The **triangular cylinder lattice** is shown in Figure A.2. It can be constructed by arranging the particles in an equilateral triangular pattern with the mesh constant L in the x,y-plane and translating the arragement by multiples of L in the z-direction. Each triangle thereby generates a triangular cylinder. Again using the integer triple (i,j,k) for the identification of each lattice point, one obtains the following formulas for the Cartesian coordinates of the points:

$$\begin{aligned} x(i,j,k) &= iL + \left|j \pmod 2\right| \frac{1}{2} L \quad , \\ y(i,j,k) &= j \frac{\sqrt{3}}{2} L \quad , \\ z(i,j,k) &= k\, L \quad . \end{aligned} \tag{A.4}$$

In a triangular cylinder lattice that occupies an infinite space the gas volume fraction is

$$\bar{\alpha} = 1 - \frac{8\pi}{3\sqrt{3}} \left(\frac{s}{L}\right)^3 \quad , \tag{A.5}$$

where s is the radius of the particles. The smallest possible value of $\bar{\alpha}$ is obtained for the largest possible value of s. Because s cannot be larger than L/2, one obtains

$$\bar{\alpha}_{min} = 1 - \pi/(3\sqrt{3}) = 0.395\ 400\ 2 \quad . \tag{A.6}$$

The **leap-frog square lattice** is shown in Figure A.3. It can be constructed by first arranging the particles in the x,y-plane in a square mesh with the mesh constant L and the square sides parallel to the coordinate axes. Then the pattern is translated by multiples of $L/\sqrt{2}$ in the z-direction and by multiples of L/2 in the x- and y-directions. Thus, each square is translated in a leap-frog manner from one z-plane to the next. The ensuing lattice is also known as "face-centered cubic lattice" with the lattice constant $2\sqrt{2}\cdot L$. Identifying each lattice point by the integer triple (i,j,k), one obtains the following expressions for the Cartesian coordinates of the points:

$$\begin{aligned} x(i,j,k) &= i\, L + \left|k \pmod 2\right| \frac{1}{2} L \quad , \\ y(ij,k) &= j\, L + \left|k \pmod 2\right| \frac{1}{2} L \quad , \\ z(i,j,k) &= k \frac{1}{\sqrt{2}} L \quad . \end{aligned} \tag{A.7}$$

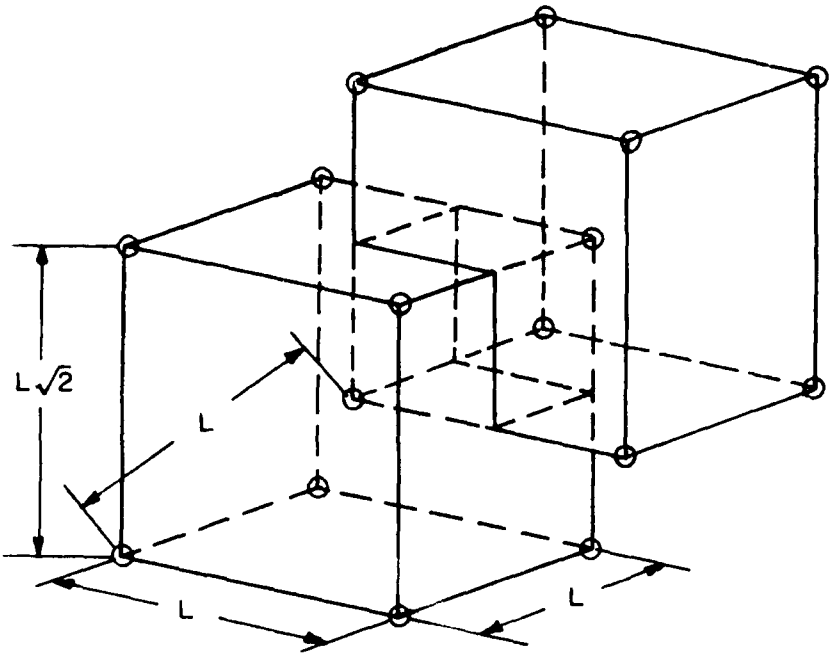

Figure A.3. Leap-Frog Square Lattice

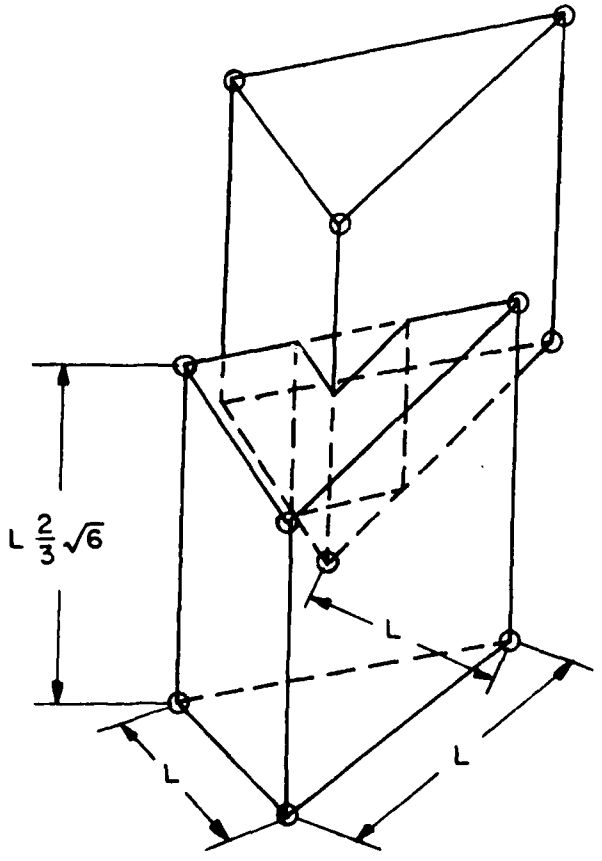

Figure A.4. Leap-Frog Triangular Lattice

If a leap-frog square lattice occupies an infinite space, then the gas volume fraction is

$$\bar{\alpha} = 1 - \frac{8\pi}{3\sqrt{2}} \left(\frac{s}{L}\right)^3 \quad . \tag{A.8}$$

Because the maximum possible value of the particle radius s is L/2, one obtains from Equation (A.8)

$$\bar{\alpha}_{min} = 1 - \pi/(3\sqrt{2}) = 0.259\ 519\ 5 \quad . \tag{A.9}$$

The leap-frog square lattice and the leap-frog triangular lattice, which we describe next, have the highest possible particle concentrations (the lowest possible $\bar{\alpha}_{min}$) of all three dimensional lattices.

The **leap-frog triangular lattice** is shown in Figure A.4. It can be constructed by first arranging the particles in the x,y-plane in an equilateral triangular mesh with the mesh constant L, as shown in Figure A.2. Then the pattern is translated in the z-direction by multiples of $\sqrt{2/3}\ L$, and in the y-direction alternatively by $\pm(\sqrt{3}/3)L$. Thus, the triangular mesh is shifted in a leap-frog manner as one proceeds from one z-plane to the next. Identifying each lattice point with the integer triple (i,j,k), one obtains the following Cartesian coordinates of the lattice points:

$$\begin{aligned} x(i,j,k) &= i\ L + \left|j \pmod 2\right| \frac{1}{2} L \quad , \\ y(i,j,k) &= j \frac{\sqrt{3}}{2} L + \left|k \pmod 2\right| \frac{\sqrt{3}}{3} L \quad , \\ z(i,j,k) &= k \sqrt{\frac{2}{3}}\ L \quad . \end{aligned} \tag{A.10}$$

The gas volume fraction $\bar{\alpha}$ in an infinite leap-frog triangular lattice can be computed by the same formula (A.8) as for the infinite leap-frog square lattice. Consequently, also the smallest possible $\bar{\alpha}_{min}$ is given by Eq. (A.9).

The formulas for $\bar{\alpha}$ have for all four lattices the form

$$\bar{\alpha} = 1 - A\ (s/L)^3 \quad , \tag{A.11}$$

where A is a constant that depends on the lattice type. Because we have defined the lattice constant L in such a manner that it is the closest distance between any two centers of particles, the minimum value of $\bar{\alpha}$ is in all cases obtained by setting s = L/2 in Eq. (A.11). Therefore,

$$A = 8\,(1 - \bar{\alpha}_{min}) = 8\,\bar{\beta}_{max} \quad , \tag{A.12}$$

where $\bar{\beta}_{max}$ is the highest possible solid volume fraction in an infinite lattice. Eliminating A between Eq. (A.11) and (A.12) one obtains

$$\bar{\alpha} = 1 - 8\,\bar{\beta}_{max}\,(s/L)^3 \tag{A.13}$$

as a general formula for $\bar{\alpha}$. The value of $\bar{\beta}_{max}$ depends, of course, on the lattice type. Table A.1 lists the values of $\bar{\alpha}_{min}$ and $\bar{\beta}_{max}$ for the four lattice types considered. The last column of the table contains the ratio of the mean distance between particle centers and the neighbor distance. That ratio is also a characteristic of each lattice. The mean distance is defined in Appendix B.

TABLE A.1. LATTICE CHARACTERISTICS

Lattice	Gas Volume Fraction $\bar{\alpha}_{min}$	Solid Volume Fraction $\bar{\beta}_{max}$	Mean Distance to Neighbor Distance $L_m/L = (\bar{\beta}_{max})^{-1/3}$
Square Cylinder	$1 - \bar{\pi}/6 = 0.476\ 401\ 2$	$\bar{\pi}/6 = 0.523\ 598\ 8$	1.240 701 0
Triangular Cylinder	$1 - \bar{\pi}/(3\sqrt{3}) = 0.395\ 400\ 2$	$\bar{\pi}/(3\sqrt{3}) = 0.604\ 599\ 8$	1.182 616 7
Leap-Frog Square	$1 - \bar{\pi}/(3\sqrt{2}) = 0.259\ 519\ 5$	$\bar{\pi}/(3\sqrt{2}) = 0.740\ 480\ 5$	1.105 338 9
Leap-Frog Triangular	$1 - \bar{\pi}/(3\sqrt{2}) = 0.259\ 519\ 5$	$\bar{\pi}/(3\sqrt{2}) = 0.740\ 480\ 5$	1.105 338 9

APPENDIX B

NEIGHBOR DISTANCE AND MEAN DISTANCE

APPENDIX B

NEIGHBOR DISTANCE AND MEAN DISTANCE

The density of a particle aggregate can be characterized by various parameters: the solid volume fraction β, the particle volume and the number density, the particle radius and a mean distance, the particle radius and a neighbor distance in a given lattice, etc. In this Appendix we discuss the concepts neighbor distance and mean distance.

As **neighbor distance** we define the smallest distance between particle centers. For the lattices defined in Appendix A the neighbor distance is equal to the lattice constant L. However, the number of neighbors with a distance L is different for different lattices. Thus, in a square cylinder lattice each particle has six nearest neighbors, in a triangular cylinder lattice the number is eight, and in the leap-frog lattices there are twelve nearest neighbors to each particle. One can also construct regular lattices in which the number of nearest neighbors is not the same for all particles.

For any of the four lattices considered in this report one can calculate for given $\bar{\alpha}$ the corresponding neighbor distance by solving Eq. (A.13) for L:

$$L = 2s \left(\bar{\beta}_{max}/(1-\bar{\alpha})\right)^{1/3} = 2s\left(\bar{\beta}_{max}/\bar{\beta}\right)^{1/3} \quad . \tag{B.1}$$

The values of $\bar{\beta}_{max}$ are given in Table A.1 for each lattice. We see from Eq. (B.1) that the neighbor distance is different for different lattices, even if s and $\bar{\alpha}$ are the same. This is not very convenient when computations are compared. Therefore, we also define a mean distance L_m that is independent of the arrangement of the particles.

Let the number of particles in the particle aggregate be m, the volume of each particle be $v(s) = (4/3)\,\pi\, s^3$, and the volume of the particle aggregate be W. One may conceptually assign to each particle the fraction W/m of the total volume and represent this fraction as a virtual sphere with the diameter L_m. This diameter we define as the mean distance between the centers of particles. A relation between the solid volume fraction β and L_m can be derived as follows. By definition one has

$$\frac{W}{m} = \frac{\pi}{6} L_m^3 \tag{B.2}$$

and the solid volume fraction in W is

$$\bar{\beta} = \frac{m\, v(s)}{W} = \frac{v(s)}{W/m} = 8\,(s/L_m)^3 \quad , \tag{B.3}$$

or

$$L_m = s/\bar{\beta}^{\,1/3} = 2s(1-\bar{\alpha})^{-1/3} \quad . \tag{B.4}$$

In Eqs. (B.3) and (B.4) we have used $\bar{\beta}$ and $\bar{\alpha}$ (the limit values) because the definition (B.2) pertains to the whole particle aggregate. We notice that the quotient W/m is the inverse of the number density of particles. Therefore, L_m is proportional to the cube root of the inverse of the number density. If we consider a finite part of the particle aggregate, defined by an averaging volume with radius R and containing N particles, then the equation corresponding to Eq. (B.2) is only approximately valid:

$$\frac{\frac{\pi}{6}\,(2R)^3}{N} \approx \frac{\pi}{6}\,L_m^3 \quad . \tag{B.5}$$

(The equation is not exactly satisfied because L_m is the mean distance for the whole particle aggregate.) Solving Eq. (B.5) for N one obtains

$$N \approx \left(\frac{2R}{L_m}\right)^3 \tag{B.6}$$

as an estimate of the number of particles in an averaging sphere. The approximation by Eq. (B.6) is quite accurate, as shown by the numerical results in Section 3. The relation (B.6) is of course independent of the particle arrangement, i.e., of the lattice type.

The advantage of the mean distance L_m over the neighbor distance L is that the former is independent of the spacial arrangement (lattice) of the particles. It is a parameter, like α, β, s and the number density, that defines a general characteristic of the particle aggregate. Because $\beta = 1-\alpha$ and because Eqs. (B.2) and (B.3) hold between these five parameters, only two of them can be prescribed for a particular aggregate. In addition to the two parameters, one may also specify a structure (lattice) of the particle arrangement, which includes a definition of a lattice constant L. The relation between the lattice constant L and the mean distance L_m is different for different lattices. For the lattices defined in Appendix A one obtains with $s_{max} = L/2$ from Eqs. (B.1) and (B.3)

$$L/L_m = 3^{1/3}_{max} \quad . \tag{B.7}$$

The value of $\bar{\beta}_{max}$ depends on the lattice type. Numerical values of the ratio L_m/L are given in Table A.1, and according to that table the mean distance in the four regular three dimensional lattices is 10% to 24% larger than the neighbor distance.

Next, we estimate the mean particle distance for interior ballistics applications. Obviously any average distance for the whole gas-particle system increases during the firing cycle, because the available volume increases due to the motion of the projectile. Let α_o be the initial gas volume fraction in the gun chamber and s_o be the initial radius of the particles. Then the initial mean distance is according to Eq. (B.4)

$$L_{mo} = 2s_o(1-\alpha_o)^{-1/3} \quad . \tag{B.8}$$

Let $z_{chamber}$ be the length of the chamber and z_{travel} be the travel of the projectile from its initial position. The ratio of the available volume W_o before and W after the projectile has moved by z_{travel} is approximately $1 + z_{travel}/z_{chamber}$. The corresponding relative increase of the mean distance L_m is according to Eq. (B.2) the cube root of this ratio. Therefore, we have the following general formula for the mean particle distance in a gun:

$$\begin{aligned} L_m &= L_{mo}(W/W_o)^{1/3} \\ &= 2s_o(1+z_{travel}/z_{chamber})^{1/3}(1-\alpha_o)^{-1/3} \end{aligned} \quad . \tag{B.9}$$

According to this equation the maximum of the mean distance is reached during a firing cycle when z_{travel} is the muzzle value. Typical numerical values in Eq. (B.9) are as follows. The initial gas volume fraction α_o is between 0.4 and 0.6, and $z_{travel}/z_{chamber} > 10$. Therefore, the maximum of the ratio $L_m/2s_o$ is for a typical gun between 2.64 and 3.02. Differently formulated, the maximum of the mean distance L_m between particle centers is for interior ballistics typically about three initial particle diameters.

APPENDIX C

ALGORITHM FOR GAS VOLUME FRACTION CALCULATION

APPENDIX C

ALGORITHM FOR GAS VOLUME FRACTION CALCULATION

The gas volume in the averaging sphere with radius R can be calculated by first computing the sum of the volumes of all particles that are located inside the sphere and subtracting the sum from the sphere's volume. For particles that are intersected by the surface of the averaging sphere one only has to add to the sum the volume of the intersection between the two spheres. Next we compute the intersection volume. According to Figure C.1 we have the following relations if two spheres intersect:

$$\begin{aligned} A + a &= D \quad , \\ A^2 + h^2 &= R^2 \quad , \\ a^2 + h^2 &= s^2 \quad . \end{aligned} \tag{C.1}$$

Eliminating h^2 and solving for A and a one obtains from Eq. (6.1)

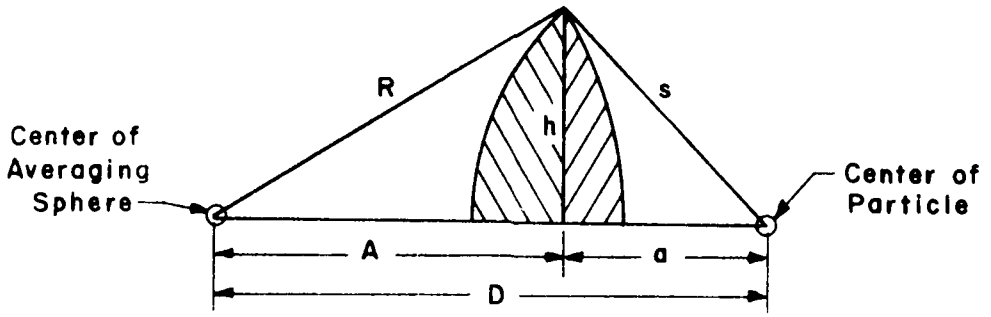

Figure C.1. Intersection of Spheres

$$\begin{aligned} A &= \frac{1}{2D}\left(D^2 + R^2 - s^2\right) \quad , \\ a &= \frac{1}{2D}\left(D^2 - R^2 + s^2\right) \quad . \end{aligned} \tag{C.2}$$

The volume of the intersection is the sum of two spherical segment volumes. The segment of the averaging sphere has the volume

$$V_R = \frac{1}{6}\pi\ (R-A)\left[3h^2 + (R-A)^2\right] = \frac{1}{3}\pi\ (R-A)^2\ (2R + A) \quad , \qquad (C.3)$$

the volume of the particle segment is

$$V_s = \frac{1}{3}\pi\ (s - a)^2\ (2s + a) \quad , \qquad (C.4)$$

and the volume of the intersection is

$$V_i = V_R + V_s \quad . \qquad (C.5)$$

The computation of the solid volume within the averaging sphere can be done as follows. First, using the given coordinates of the center of the sphere and the specifications of the lattice, one defines a search area in terms of minimum and maximum values of the integers (i,j,k) (see Appendix A). Next, one computes for each lattice point within the search area the distance D between the point and the center of the averaging sphere. If $D > R + s$, then the particle is outside the averaging sphere. If $D < |R - s|$, then one of the two spheres (averaging sphere and particle) is inside the other, depending on which one is bigger. Then the solid volume is equal to the smaller of the two sphere volumes. Finally, if $|R-s| < D < R+s$, then the intersection volume is calculated by the formulas (C.2) through (C.5) and added to the sum of solid volumes that are located inside the averaging sphere.

APPENDIX D

GAS VOLUME FRACTION AT A PARTICLE AGGREGATE BOUNDARY

APPENDIX D

GAS VOLUME FRACTION AT A PARTICLE AGGREGATE BOUNDARY

Let a particle aggregate with the limit gas volume fraction $\bar{\alpha}$ occupy the half-space $z \geq 0$. Our goal is to obtain an approximate transition of the gas volume fraction from $\alpha = 1$ at large negative values of z to $\alpha \approx \bar{\alpha}$ at large positive values of z. In order to derive the approximation we assume that the gas volume fraction can be approximated by $\bar{\alpha}$ in that part of the averaging sphere that intersects with the half-space $z \geq 0$. Under this assumption α is only a function of the coordinate z_c of center of the averaging sphere. Our goal is to find that function.

We notice that the assumption about the approximation of α by $\bar{\alpha}$ cannot be realized in any real particle aggregate. The undulations of α about $\bar{\alpha}$ can be reduced to arbitrarily low levels if R/L_m is sufficiently large, but only if the whole averaging sphere is within the half-space $z \geq R$. If the averaging sphere is allowed to intersect partly with the half-space $z \geq 0$, then the intersecting volume cannot be assumed always large, even if $R/L_m \gg 1$, and, therefore, the undulations are only bounded by $|\Delta\alpha| \leq \max(\bar{\alpha}, 1-\bar{\alpha})$.

Let z_c be the z-coordinate of the center of the averaging sphere. The volume of the intersection of the sphere with the half-space $z \geq 0$ is

$$V_{\bar{\alpha}} = \begin{cases} 0 & , \quad \text{if} \quad z_c \leq -R \quad , \\ \frac{\pi}{3}\left(R + z_c\right)^2(2R - z_c) & , \quad \text{if} \quad -R < z_c < R \quad , \\ \frac{4}{3}\pi R^3 & , \quad \text{if} \quad R \leq z_c \quad . \end{cases} \tag{D.1}$$

Because we assume that $\alpha = \bar{\alpha}$ in any finite part of the half-space $z > 0$, the gas volume fraction in the averaging sphere is

$$\begin{aligned} \alpha &= \frac{1}{V_R}\left(V_{\bar{\alpha}} \cdot \bar{\alpha} + \left(V_R - V_{\bar{\alpha}}\right) \cdot 1\right) = \\ &= 1 - (1 - \bar{\alpha})\, V_{\bar{\alpha}}/V_R \end{aligned} \tag{D.2}$$

where $V_R = (4/3)\,\pi\, R^3$ is the volume of the averaging sphere. Combining Eqs. (D.1) and (D.2) one obtains

$$\alpha(z_c) = \begin{cases} 1 & , \text{ if } z_c < -R \\ 1-(1-\bar{\alpha})\ (1 + z_c/R)^2\ (2 - z_c/R)/ & , \text{ if } -R < z_c < -R \\ \bar{\alpha} & , \text{ if } R < z_c \end{cases} \quad , \quad (D.3)$$

The limit of the transition curve for $R/L_m \to \infty$ is simply $\alpha \equiv (1+\bar{\alpha})/2$. This is a nice illustration to the smoothing effect of averaging: If the averaging volume is made so large that the particle-induced heterogeneities are zero, then also all flow structures (aggregate boundary in the present example) are reduced to constants.

APPENDIX E

UNDULATIONS OF AVERAGE FUNCTIONS

APPENDIX E

UNDULATIONS OF AVERAGE FUNCTIONS

Let $\check{\phi}$ be a local gas property, for instance, density. Then the corresponding average ϕ is defined by

$$\phi = \frac{1}{V_{gas}} \int_{V_{gas}} \check{\phi}\, dV \quad , \tag{E.1}$$

where V_{gas} is that part of the averaging volume V which is occupied by gas. If $\check{\phi}$ is constant, then obviously $\phi \equiv \check{\phi}$ for any positive value of $V_{gas} = \alpha V$. If $\check{\phi}$ is not constant, then the particles in V influence the value of the average ϕ, that is, ϕ depends in such a case on α. Particularly, if α undulates, then also ϕ undulates. We estimate the amplitude $\Delta\phi$ of the undulations for a local function $\check{\phi}$ with a constant gradient. We assume without loss of generality that only the x-component of the gradient is non-zero and express $\check{\phi}$ by

$$\check{\phi}(x,y,z) = \check{\phi}_o + (x-x_o)\,\check{\phi}_x \tag{E.2}$$

with constant $\check{\phi}_o$, x_o and $\check{\phi}_x$. The corresponding average value is obtained by substituting the expression (E.2) into the integral (E.1). Let the particle volumes v be all equal and small compared to the averaging volume V, let x denote the x-coordinate of the center of V, and x_i, i=1,...,N, denote the centers of the N particles that are inside the averaging volume V. Then the average value of $\check{\phi}$ is approximately equal to

$$\begin{aligned}
\phi(x) &= \frac{1}{V-\Sigma v}\left\{V\left[\check{\phi}_o+(x-x_o)\check{\phi}_x\right] - \sum_1^N v\left[\check{\phi}_o+(x_i-x_o)\check{\phi}_x\right]\right\} \\
&= \frac{1}{V-Nv}\left\{(V-Nv)\left[\check{\phi}_o-(x-x_o)\check{\phi}_x\right] - v\,\check{\phi}_x \sum_1^N (x_i-x)\right\} \\
&= \check{\phi}_o + (x-x_o)\,\check{\phi}_x - \check{\phi}_x\bar{\xi}\,(1-\alpha)/\alpha
\end{aligned} \tag{E.3}$$

where $\bar{\xi}$ is the average deviation of the particle positions from the center of V.

Next we relocate the averaging volume to the position $x+\Delta x$. The relocation affects the average value of $\check{\phi}$ in two ways. First, the local function is averaged over a different region and the positions of the N particles have changed relative to V. According to Eq. (E.3) this changes

the average by

$$\Delta x \cdot \tilde{\phi}_x (1 + (1-\alpha)/\alpha) \quad . \tag{E.4}$$

A second effect is due to a possible change of the number of particles within V. Let ΔM be the number of particles that have been added by the relocation and Δm be the number of particles that have been lost by the relocation. The total number of particles within V then changes by

$$\Delta N = \Delta M - \Delta m \tag{E.5}$$

and the gas volume fraction changes by

$$\Delta\alpha = -\frac{v}{V}\Delta N = -(1-\alpha)\Delta N/N \quad . \tag{E.6}$$

The average value of $\tilde{\phi}$ at $x+\Delta x$ is, with the same approximation as Eq. (E.3),

$$\begin{aligned}
\phi(x+\Delta x) &= \frac{1}{V-(N+\Delta N)v_p}\left\{V\left[\tilde{\phi}_o + (x+\Delta x-x_o)\tilde{\phi}_x\right] - \right. \\
&\left. - v\left(\sum^{N} + \sum^{\Delta M} - \sum^{\Delta m}\right)\left[\tilde{\phi}_o + (x_i - x_o)\,\tilde{\phi}_x\right]\right\} = \\
&= \frac{1}{V-(N+\Delta N)v}\left\{\left[V-(N+\Delta N)v\right]\left[\tilde{\phi}_o + (x+\Delta x-x_o)\tilde{\phi}_x\right] - \right. \\
&\left. - v\tilde{\phi}_x\left(\sum^{N} + \sum^{\Delta M} - \sum^{\Delta m}\right)\left[x_i - x - \Delta x\right]\right\} = \\
&= \tilde{\phi}_o + (x+\Delta x-x_o)\,\tilde{\phi}_x - \\
&- \frac{1-\alpha}{\alpha+\Delta\alpha}\,\tilde{\phi}_x\left[\bar{\xi}-\Delta x + \frac{1}{N}\left(\sum^{\Delta M} - \sum^{\Delta m}\right)(x_i - x - \Delta x)\right] \quad .
\end{aligned} \tag{E.7}$$

We consider the last term in Eq. (E.7) and observe that the particles are added and removed at opposite sides of the averaging volume. If V is a sphere with radius R, then one may estimate the average x-coordinates of the added particles by $\bar{x}_i \approx x + 2R/3 + \Delta x/2$ and the corresponding average of the coordinates of the lost particles by $\bar{x}_i \approx x - 2R/3 + \Delta x/2$. Then the last term in Eq. (E.7) is

$$\frac{1}{N}\sum^{\Delta M}(x_i - x - \Delta x) - \frac{1}{N}\sum^{\Delta m}(x_i - x - \Delta x) \approx$$

$$\approx \frac{1}{N}\Delta M(2R/3 - \Delta x/2) + \frac{1}{N}\Delta m(2R/3 + \Delta x/2) = \qquad \text{(E.8)}$$

$$= \frac{1}{N}\frac{2}{3}R(\Delta M + \Delta m) - \frac{1}{N}\frac{\Delta x}{2}(\Delta M - \Delta m) \quad .$$

Next we express ΔM and Δm in terms of α and $\Delta\alpha$. The region of space newly covered by the relocation of V has the volume

$$\Delta V = \pi R^2 \Delta x = V\frac{3\Delta x}{4R} \qquad \text{(E.9)}$$

and an equal volume is abandoned. Let α_M be the average value of α in the added region and α_m be the average value in the abandoned region. Then the numbers of added and lost particles are

$$\left.\begin{aligned} \Delta M &= (1-\alpha_M)\frac{\Delta V}{v} = (1-\alpha_M)\frac{V}{v}\frac{3\Delta x}{4} = \frac{1-\alpha_M}{1-\alpha}N\frac{3\Delta x}{4R} \\ \text{and} \qquad & \\ \Delta m &= (1-\alpha_m)\frac{\Delta V}{v} = \frac{1-\alpha_m}{v} = \frac{1-\alpha_m}{1-\alpha}N\frac{3\Delta x}{4R} \quad . \end{aligned}\right\} \text{(E.10)}$$

Substituting these values into Eq. (E.8), one obtains the expression

$$\frac{1-\alpha_M+1-\alpha_m}{2(1-\alpha)}\Delta x + \frac{3\Delta x}{8R}\frac{\alpha_M-\alpha_m}{1-\alpha} \quad . \qquad \text{(E.11)}$$

If the gas volume fraction is uniform ($\alpha_M \approx \alpha_m \approx \alpha$), then this expression is equal to Δx. We assume that α is not uniform, particularly that α is increased by $\Delta\alpha$ due to an excess of added particles over the average ΔM in Eq. (E.10). We express this assumption by modifying Eq. (E.10) to

$$\left.\begin{aligned} \Delta M &= (1-\alpha)\frac{\Delta V}{v} + \Delta N = N\frac{3}{4R}\Delta x + \Delta N \\ \text{and} \qquad & \\ \Delta m &= (1-\alpha)\frac{\Delta V}{v} \qquad = N\frac{3}{4R}\Delta x \quad . \end{aligned}\right\} \text{(E.12)}$$

Then the expression Eq. E.8) becomes equal to

$$\Delta x + \frac{1}{N}\frac{2R}{3}\Delta N - \frac{1}{N}\Delta x \frac{1}{2}\Delta N \quad . \tag{E.13}$$

Replacing the last term in Eq. (E.7) by this expression we obtain

$$\phi(x+\Delta x) = \tilde{\phi}_o + (x+\Delta x - x_o)\tilde{\phi}_x - \tag{E.14}$$

$$- \frac{1-\alpha}{\alpha+\Delta\alpha}\tilde{\phi}_x\left[\bar{\xi} + \frac{\Delta N}{N}\left(\frac{2R}{3} - \frac{\Delta x}{2}\right)\right] \quad ,$$

or, using Eq. (E.6)

$$\phi(x+\Delta x) = \tilde{\phi}_o + (x+\Delta x - x_o)\,\tilde{\phi}_x \tag{E.15}$$

$$- \frac{1-\alpha}{\alpha+\Delta\alpha}\tilde{\phi}_x\left[\bar{\xi} - \frac{\Delta\alpha}{1-\alpha}\frac{2R}{3}\left(1 - \frac{3}{2}\,\frac{\Delta x}{2R}\right)\right] \quad .$$

The difference between Eqs. (E.3) and (E.15) is

$$\phi(x+\Delta x) - \phi(x) = \Delta x\,\tilde{p}_x \tag{E.16}$$

$$- \frac{1}{\alpha+\Delta\alpha}\tilde{\phi}_x\,\frac{2R}{3}\,\Delta\alpha\left[1 - \frac{3}{2}\,\frac{\Delta x}{2R} + \frac{1-\alpha}{\alpha}\,3\,\frac{\bar{\xi}}{2R}\right] \quad .$$

Hence the change of the average function ϕ due to a change of α is

$$C = -2R\tilde{\phi}_x\,\frac{\Delta\alpha}{3(\alpha+\Delta\alpha)}\left[1 - \frac{3}{2}\,\frac{\Delta x}{2R} + \frac{1-\alpha}{\alpha}\,3\,\frac{\bar{\xi}}{2R}\right] \quad . \tag{E.17}$$

In order to estimate the amplitude of the undulations of ϕ we set Δx equal to about one fourth of the wave length of the undulations of α. According to Section 4 the wave length is between 1.0 and 1.5 L_m. By setting $\Delta x = L_m/3$ in Eq. (E.17) we obtain

$$C \approx -2R\breve{\phi}_x \frac{\Delta\alpha}{3(\alpha+\Delta\alpha)}\left[1 - \frac{L_m}{4R} + \frac{1-\alpha}{\alpha}\,3\,\frac{\bar{\xi}}{2R}\right] \quad . \tag{E.18}$$

The quantity $|2R\breve{\phi}_x|$ is the maximum change of the local gas property $\breve{\phi}$ along a diagonal of the averaging volume. According to Eq. (E.16) this is also the change of the average function ϕ if undulations are not present. Let that change be denoted by $\delta\phi$. The term $L_m/4R$ in Eq. (E.18) can be assumed less than 0.25 or smaller. Also, $|\bar{\xi}| \ll 2R$, so that the two terms involving L_m and $\bar{\xi}$ can be neglected in our estimate of C. If we also assume $|\Delta\alpha| \ll \alpha$, then Eq. (E.18) yields the following estimate for the amplitude $\Delta\phi$ of the undulations of ϕ:

$$\Delta\phi \approx |\delta\phi||\Delta\alpha|/(3\alpha) \quad . \tag{E.19}$$

A corresponding estimate with $1-\alpha$ replacing α can be obtained for the average properties of particles, which are defined by

$$\phi = \frac{1}{V_{partc.}} \int_{V_{partc.}} \breve{\phi}\, dV \tag{E.20}$$

where V_{partc} is that part of the averaging volume which is occupied by particles and $\breve{\phi}$ is a local particle property.

Undulations of α also can affect such average functions which have a zero gradient ($\delta\phi=0$), if the local property $\breve{\phi}$ is affected by the presence of particles. One example of such a situation is a particle aggregate that moves with velocity $\overset{*}{u}$ through a quiescent viscous gas. Then the average gas velocity in a large averaging volume is not zero but approximately a fraction of $\overset{*}{u}$. The size of the fraction depends on the thickness of the boundary layer around each particle and on the number of particles, that is, on α. A similar example is the average temperature of a gas in which one places particles with a different temperature. We notice that in the latter example the average gas temperature undulates with an amplitude proportional to the undulations of α, whereas the average particle temperature is affected only by higher order terms. We demonstrate this remark by considering the following simple model in which the gas has a constant property $\breve{\phi}_b$ in a boundary region around each particle and a constant property $\breve{\phi}_o$ elsewhere in the flow field. The volume of the boundary region around a particle we denote by $v\varepsilon$. (For a spherical particle with radius s and boundary region thickness $\Delta s \ll s$ one has $\varepsilon = 3\Delta s/s$.) Then the average gas property ϕ is

$$\phi = \frac{1}{V-Nv}\left[(V-Nv - Nv\,\varepsilon)\,\tilde{\phi}_o + Nv\,\varepsilon\tilde{\phi}_b\right] \quad ,$$

$$= \frac{1}{\alpha}\left[(\alpha - (1-\alpha)\,\varepsilon)\,\tilde{\phi}_o + (1-\alpha)\,\varepsilon\tilde{\phi}_b\right] \quad , \qquad \text{(E.21)}$$

$$= \tilde{\phi}_o + (\tilde{\phi}_b - \tilde{\phi}_o)\,\varepsilon\,(1-\alpha)/\alpha \quad .$$

Because the average ϕ depends on α, undulations of α will cause undulations of ϕ. For small undulations $\Delta\alpha << \alpha$ one obtains from Eq. (E.21) the estimate

$$\Delta\phi = -(\tilde{\phi}_b - \tilde{\phi}_o)\,\varepsilon\,\Delta\alpha/\alpha^2 \quad , \qquad \text{(E.22)}$$

that is, $\Delta\phi$ is proportional to $\Delta\alpha$. The average particle properties are not affected by $\Delta\alpha$ under similar conditions. Let $\tilde{\psi}_b$ be a constant particle property in a boundary region within each particle, and $\tilde{\psi}_o$ be a constant particle property elsewhere in the particles. The average ψ then is

$$\psi = \frac{1}{Nv}\left[(Nv - Nv\,\varepsilon)\,\tilde{\psi}_o + Nv\,\varepsilon\,\tilde{\psi}_b\right]$$

$$= \frac{1}{1-\alpha}\left[(1-\alpha - (1-\alpha)\varepsilon)\,\tilde{\psi}_o + (1-\alpha)\varepsilon\tilde{\psi}_b\right] \qquad \text{(E.23)}$$

$$= \tilde{\psi}_o + (\tilde{\psi}_b - \tilde{\psi}_o)\varepsilon \quad .$$

Because the average ψ is independent of α, it is not affected by undulations of α.

To summarize, we observe that if particle induced undulations of average flow properties do occur, then they likely are proportional to the undulations $\Delta\alpha$ of the gas volume fraction.

DISTRIBUTION LIST

No. of Copies	Organization
12	Administrator Defense Technical Info Center ATTN: DTIC-DDA Cameron Station Alexandria, VA 22314
1	Office of the Under Secretary of Defense Research & Engineering ATTN: R. Thorkildsen The Pentagon Washington, DC 20301
1	Commandant US Army War College ATTN: Library-FF229 Carlisle Barracks, PA 17013
1	Commander Ballistic Missile Defense Advanced Technology Center P.O. Box 1500 Huntsville, AL 35807
1	Commander US Army Materiel Development and Readiness Command ATTN: AMCDRA-ST 5001 Eisenhower Avenue Alexandria, VA 22333
3	Commander US Army Armament R&D Cmd ATTN: SMCAR-TDC SMCAR-TSS J. Lannon Dover, NJ 07801
1	Commander US Army Armament, Munitions and Chemical Command ATTN: AMSMC-LEP-L Rock Island, IL 61299
1	Commander USA Aviation Research and Dev Cmd ATTN: AMSAV-E 4300 Goodfellow Blvd. St. Louis, MO 63120
1	Director USA Air Mobility Rsch and Dev Lab Ames Research Center Moffett Field, CA 94035
1	Commander US Army Communications Research and Dev Command ATTN: AMSEL-ATDD Fort Monmouth, NJ 07703
1	Commander US Army Electronics Rsch and Dev Cmd Technical Support Act ATTN: AMDSD-L Fort Monmouth, NJ 07703
1	Commander US Army Harry Diamond Lab ATTN: DELHD-TA-L 2800 Powder Mill Road Adelphi, MD 20783
1	Commander US Army Missile Cmd ATTN: AMSMI-R Redstone Arsenal, AL 35898
1	Commander US Army Tank Automotive Command ATTN: AMSTA-TSL Warren, MI 48090
1	Director USA AMCCOM Benet Weapons Laboratory ATTN: SMCAR-LCB-TL Watervliet, NY 12189
1	US Army Tank Automotive Command ATTN: AMSTA-CG Warren, MI 48090
1	Commander US Army Missile Cmd ATTN: AMSMI-YDL Redstone Arsenal, AL 35898

DISTRIBUTION LIST

No. of Copies	Organization
1	President US Army Armor & Engineer Board ATTN: STEBB-AD-S Fort Knox, KY 40121
1	Commandant US Army Infantry School ATTN: ATSH-CD-CSO-OR Fort Benning, GA 31905
1	Director US Army TRADOC Systems Analysis Activity ATTN: ATAA-SL White Sands Missile Range NM 88002
2	Commander US Army Materials and Mechanics Rsch Center ATTN: AMXMR-ATL Tech Library Watertown, MA 02172
2	Commander US Army Research Office ATTN: Tech Library J. Chandra P.O. Box 12211 Research Triangle Park, NC 27709
1	Commander US Army Mobility Equipment Research & Development Command ATTN: AMDME-WC Fort Belvoir, VA 22060
2	Commandant US Army Infantry School ATTN: Infantry Agency Fort Benning, GA 31905
1	Commandant US Army Aviation School ATTN: Aviation Agency Fort Rucker, AL 36360
1	HQDA DAMA-ART-M Washington, DC 20310

No. of Copies	Organization
1	Commandant US Army Command and General Staff College Fort Leavenworth, KS 66027
1	Commandant US Army Special Warfare School ATTN: Rev & Tng Lit Div Fort Bragg, NC 28307
1	Commandant US Army Engineer School Fort Belvoir, VA 22060
1	Commander US Army Foreign Science & Technology Center ATTN: AMXST-MC-3 220 Seventh Street, NE Charlottesville, VA 22901
1	President US Army Artillery Board Fort Sill, OK 73503
1	Office of Naval Rsch ATTN: Code 473 R.S. Miller 800 N. Quincy Street Arlington, VA 22217
1	Commander Naval Air Systems Command ATTN: NAIR-954 Tech Lib Washington, DC 20360
2	Commander Naval Surface Weapons Center ATTN: T.P. Consaga C. Gotzmer Indian Head, MD 20640
1	Commander US Army Development & Employment Agency ATTN: MODE-TED-SAB Fort Lewis, WA 98433

DISTRIBUTION LIST

No. of Copies	Organization
1	Commander Naval Surface Weapons Center ATTN: Code 730 Silver Spring, MD 20910
1	Commander Naval Underwater Systems Center Energy Conversion Dept. ATTN: Tech Lib Newport, RI 02840
1	Commander Naval Weapons Center ATTN: Info. Science Div. China Lake, CA 93555
2	Superintendent Naval Postgraduate School Dept. of Mechanical Engineering ATTN: A.E. Fuhs, Code 1424 Library Monterey, CA 93940
2	Commander Naval Ordnance Station ATTN: Tech Library W. Rogers Indian Head, MD 20640
1	AFSC/SDOA Andrews AFB, MD 20334
1	Commander Naval Surface Weapons Center ATTN: Code DX-21 Tech Library Dahlgren, VA 22448
1	AFATL ATTN: DLYV Eglin AFB, FL 32542
1	ADTC ATTN: DLODL Tech Lib Eglin AFB, FL 32542
1	AFWL/SUL Kirtland AFB, NM 87117
1	Atlantic Research Corp. ATTN: M.K. King 5390 Cherokee Ave. Alexandria, VA 33214
1	AFATL/DLDL ATTN: O.K. Heiney Eglin AFB, FL 32542
1	Brigham Young University Department of Chemical Eng ATTN: M. Beckstead Provo, UT 84601
2	Calspan Corporation ATTN: E.B. Fisher, Tech Library P.O. Box 400 Buffalo, NY 14225
1	AFOSR Directorate of Aerospace Sciences ATTN: L.H. Caveny Bolling AFB, DC 20332
1	AFRP L(DYSC) ATTN: Tech Library Edwards AFB, CA 93523
1	AFFTC AFRPL/LKCG ATTN: SSD-Tech Lib Edwards AFB, CA 93523

DISTRIBUTION LIST

No. of Copies	Organization
1	Director Jet Propulsion Laboratory 4800 Oak Grove Drive Pasadena, CA 91109
1	University of Massachusetts Dept. of Mechanical Engineering ATTN: K. Jakus Amherst, MA 01002
1	University of Minnesota Dept. of Mechanical Engineering ATTN: E. Fletcher Minneapolis, MN 55455
1	Case Western Reserve University Division of Aerospace Sciences ATTN: J. Tien Cleveland, OH 44135
1	United Technologies Chemical Systems Division ATTN: Tech Library P.O. Box 358 Sunnyvale, CA 94086
1	Battelle Memorial Inst. ATTN: Tech Library 505 King Avenue Columbus, OH 43201
1	Johns Hopkins University Applied Physics Lab Chemical Propulsion Information Agency ATTN: T. Christian Johns Hopkins Road Laurel, MD 20707
1	Massachusetts Institute of Technology Department of Mechanical Engineering ATTN: T. Toong 170 Albany St. Cambridge, MA 02139
1	Pennsylvania State Univ. Dept. of Mech. Eng. ATTN: K.K. Kuo University Park, PA 16802
1	Massachusetts Inst. of Tech Dept. of Materials Sciences and Engineering ATTN: J. Szekely 77 Massachusetts Ave Cambridge, MA 02139
1	California Institute of Tech 204 Karman Lab Main Stop 301-46 ATTN: F.E.C. Culick 1201 E. California Street Pasadena, CA 91125
1	University of Illinois-Urbana Mechanics and Industrial Eng. ATTN: S.L. Soo Urbana, IL 61801
1	University of Maryland Inst of Physical Sciences and Technology ATTN: S.I. Pai College Park, MD 20740
2	University of Wisconsin-Madison Mathematics Resch Center ATTN: J.R. Bowen Tech Library 610 Walnut Street Madison, WI 53706
1	Worcester Polytechnic Institute Dept. of Mathematics ATTN: P.W. Davis Worcester, MA 01609
1	Pennsylvania State Univ. Applied Research Lab ATTN: G.M. Faeth University Park, PA 16802

DISTRIBUTION LIST

No. of Copies	Organization
2	University of Utah Dept. of Chem. Eng. ATTN: A. Baer C. Flandro Salt Lake City, UT 84112
1	Washington State Univ. Dept. of Mechanical ATTN: C.T. Crowe Pullman, WA 99163
2	Lawrence Livermore ATTN: M.S. L-355 A. Buckingham M. Finger P.O. Box 808 Livermore, CA 94550
1	University of Kentucky Dept. of Mech. Engineering ATTN: M.C. Roco Lexington, KY 40506
1	Stevens Institute of Technology ATTN: F. Dobran Hoboken, NJ 07030
2	Carnegie-Mellon University Dept. of Mathematics ATTN: George Fix M. Gunzburger Pittsburgh, PA 15213
3	Georgia Institute of Technology School of Aerospace Eng. ATTN: B.T. Zinn E. Price W.C. Strahle Atlanta, GA 30332
1	Institute of Gas Technology ATTN: D. Gidaspow 3424 S. State Street Chicago, IL 60616
1	University of Cincinnati Department of Aerospace Engineering ATTN: W. Tabakoff Cincinnati, OH 45221
1	University of Delaware Department of Mathematical Sciences ATTN: M.Z. Nashed Newark, DE 19711
1	University of Illinois College of Engineering Department of Aeronautical and Astronautical Engineering ATTN: H. Krier Urbana, IL 61801
1	Massachusetts Institute of Technology Department of Mathematics ATTN: H.P. Greenspan 77 Massachusetts Ave. Cambridge, MA 02139
1	University of Cincinnati ATTN: A. Hamed Cincinnati, OH 45221
1	Rensselaer Polytechnic Inst. Mathematical Science Dept. ATTN: D. Drew Troy, NY 12181
1	Rutgers University Dept. of Mechanical and Aerospace Engineering ATTN: S. Temkin Univ. Heights Campus New Brunswick, NJ 08903
1	SRI International Propulsion Sciences Division ATTN: Tech Library 333 Ravenswood Avenue Menlo Park, CA 94025

DISTRIBUTION LIST

No. Of Copies	Organization
1	University of Southern Calif. Dept. of Mechanical Eng. ATTN: OHE200 C. Gerstein Los Angelos, CA 90007
3	Los Alamos National Laboratory ATTN: Thomas Butler MS B216 M. Davision B. Craig P.O. Box 1663 Los Alamos, NM 87544
1	Purdue University School of Mechanical Engineering ATTN: J.R. Osborne TSPC Chaffee Hall West Lafayette, IN 47906
1	Science Applications, Inc. ATTN: R.B. Edelman 23146 Cumorah Crest Woodland Hills, CA 91364
1	Princeton Combustion Research Laboratory, Inc. ATTN: M. Summerfield 475 US Highway One Princeton, NY 08852
1	Paul Gough Assoc., Inc ATTN: P.S. Gough 1048 South St. Portsmouth, NH 03811
1	Argonne National Laboratory Reactor Analysis and Safety Division ATTN: M. Ishii 9700 South Cass Avenue Argonne, IL 60439
1	Stevens Inst of Tech Davidson Laboratory Castle Point Station ATTN: R. McAlevy, III Hoboken, NJ 07030
4	Los Alamos Scientific Laboratory ATTN: GROUP T-7 B. Wendroff D. Durak W.H. Lee Los Alamos, NM 87544
3	Scientific Research Assoc., Inc. ATTN: H. McDonald H.F. Gibeling R.C. Buggeln P.O. Box 498 Glastonbury, CT 06033

Aberdeen Proving Ground

Dir, USAMSAA
ATTN: AMXSY-D
AMXSY-MP,
H. Cohen

Cdr, USATECOM
ATTN: AMSTE-TO-F

Dir, USA MTD
ATTN: STEAP-MT-A
C. Herud
H. Bechtol

Cdr, CRDC, AMCCOM
ATTN: SMCCR-RSP-A
SMCCR-MU
SMCCR-SPS-IL

USER EVALUATION SHEET/CHANGE OF ADDRESS

This Laboratory undertakes a continuing effort to improve the quality of the reports it publishes. Your comments/answers to the items/questions below will aid us in our efforts.

1. BRL Report Number _____ Date of Report _____

2. Date Report Received _____

3. Does this report satisfy a need? (Comment on purpose, related project, or other area of interest for which the report will be used.) _____

_____

_____

4. How specifically, is the report being used? (Information source, design data, procedure, source of ideas, etc.) _____

_____

_____

5. Has the information in this report led to any quantitative savings as far as man-hours or dollars saved, operating costs avoided or efficiencies achieved, etc? If so, please elaborate. _____

_____

_____

6. General Comments. What do you think should be changed to improve future reports? (Indicate changes to organization, technical content, format, etc.)

_____

_____

_____

CURRENT ADDRESS

_____
Name

_____
Organization

_____
Address

_____
City, State, Zip

7. If indicating a Change of Address or Address Correction, please provide the New or Correct Address in Block 6 above and the Old or Incorrect address below.

OLD ADDRESS

_____
Name

_____
Organization

_____
Address

_____
City, State, Zip

(Remove this sheet along the perforation, fold as indicated, staple or tape closed, and mail.)

FOLD HERE

Director
US Army Ballistic Research Laboratory
ATTN: AMXBR-OD-ST
Aberdeen Proving Ground, MD 21005-5066

NO POSTAGE
NECESSARY
IF MAILED
IN THE
UNITED STATES

OFFICIAL BUSINESS
PENALTY FOR PRIVATE USE, $300

BUSINESS REPLY MAIL
FIRST CLASS PERMIT NO 12062 WASHINGTON, DC
POSTAGE WILL BE PAID BY DEPARTMENT OF THE ARMY

Director
US Army Ballistic Research Laboratory
ATTN: AMXBR-OD-ST
Aberdeen Proving Ground, MD 21005-9989

FOLD HERE

END

FILMED

2-85

DTIC